Pion Exchange Currents in Deuteron Photodisintegration. Dispersion Theory*†

MALCOLM H. SKOLNICK‡
Institute for Advanced Study, Princeton, New Jersey
(Received 20 December 1963; revised manuscript received 2 April 1964)

A dispersion-theoretic treatment of the amplitudes describing photomagnetic disintegration of the deuteron at energies very near threshold has been developed. The effects of meson exchange currents in the photodisintegration or equivalent *n-p* capture process are calculated. At threshold the photomagnetic transition is dominant. This transition is essentially the isovector $^3S_0 \rightarrow {}^1S_0$ transition. A fixed-angle dispersion relation for the dipole amplitude describing this transition can be written in terms of the related covariant amplitudes. Solutions to the dispersion relation are found using several different approximations. First, one may neglect all high-order effects which serve to define the unphysical cut, and consider only the contribution from the Born poles. Next, one may condense all the higher-order effects into a single interaction pole. The single experimental cross section value for thermal neutrons may be used to relate the position and residue of this pole in a single functional relationship by recalculating the solution to the dispersion relation with this pole included. Finally one may treat the contribution of the pion exchange currents using the Mandelstam representation, and recalculate the dispersion relations once again. This latter treatment is based upon the approximation that only the anomalous tip of the spectral function is effective in providing modifications in the physical region close to threshold. It is shown that the pion exchange terms are the dominant contributors to the spectral function in the anomalous region. The solution obtained in this approximation yields a cross section which is in agreement with the experimental value.

1. INTRODUCTION

STUDY of the electromagnetic structure of elementary particles has developed useful techniques applicable in the study of strong interactions. In examining photon or electron scattering with large momentum transfers from an otherwise strongly interacting particle, it should be possible to probe the electromagnetic structure of this particle, and learn something about the strong interactions that produce it.[1]

One may utilize the observed static moments of nucleons in scattering calculations and thus provide a partial account of exchange current effects. However, there is evidence that this partial explanation of exchange effects is not even qualitatively good enough. This could be foreseen if one would conjecture that the meson current associated with free nucleons is modified in an important way by the proximity of other nucleons. Some of these modifications are to be found in observations of the magnetic moments of two- and three-body nuclei. The magnetic moments of such nuclei are not equal to the sum of the static (free) moments of the constituent nucleons. The magnetic moments of H^3 and He^3 differ from what may be calculated when one neglects exchange interaction effects, and they exhibit a symmetry that is suggestive of exchange currents.[2] Also, the $n-p$ photomagnetic capture cross section at threshold shows a 10% discrepancy between the experimental and theoretical values.

In a calculation designed to clarify the role of exchange currents, we utilize the electromagnetically indicative properties of the pion current in as simple as possible a scattering process involving two or more nucleons.

In this effort we note that magnetic transitions should be more strongly affected by exchange effects than electric ones, since average meson velocities are higher than nucleon velocities and magnetic transitions depend on current distributions, whereas electric transitions depend on charge distributions.[3]

We also rely on experimental evidence and other corroborative calculations. In this light we suggest that a study of the photomagnetic $n-p$ capture process noted above may prove useful. This process or its inverse—deuteron photodisintegration—seems to involve all the elements and relations we have cited as useful in the study of exchange currents and the modifications imposed by nucleon proximities.

We have calculated deuteron photodisintegration, or the equivalent inverse reaction, $n-p$ capture, by applying dispersion relations to the process. There have been several efforts made to provide a covariant description of the deuteron photodisintegration process.[4–6] We follow the earlier definitive work of Sakita and Goebel (henceforth referred to as SG), who established much of the formalism appropriate to this problem. It is adapted from the covariant formalism as developed by Mandelstam *et al.* The theory is relativistic in nature, but has the advantage that some of the kinematics can be approximated nonrelativistically without forcing a like approximation in the meson dynamics.

* Submitted as a thesis in partial fulfillment of the requirements for the degree of Doctor of Philosophy at Cornell University, Ithaca, New York.
† This work was supported in part by the U. S. Office of Naval Research.
‡ On leave from Educational Services Inc., Watertown, Massachusetts. Present address: MIT, Physics Department, Cambridge, Massachusetts.
[1] G. Chew, *S-Matrix Theory of the Strong Interactions* (W. A. Benjamin and Company, New York, 1961).
[2] A. Arking, thesis, Cornell University, 1959 (unpublished).
[3] L. Eisenbud and E. P. Wigner, *Nuclear Structure* (Princeton University Press, Princeton, New Jersey, 1958).
[4] B. Sakita, thesis, University of Rochester, 1962 (unpublished); B. Sakita and C. Goebel, Phys. Rev. **127**, 1787 (1962).
[5] A. Donnachie, Nucl. Phys. **37**, 594 (1962).
[6] M. Le Bellac, F. M. Renard, and J. Tran Thanh Van (unpublished).

The framework allows incorporation of much experimental detail in calculation of the singularity structure that is difficult to accommodate in a simply related context in potential theory.

Briefly, the procedure is such that one associates the external particles involved in the process with local fields in the conventional sense. One then constructs or reconstructs trilinear interactions describing each vertex. These interactions are constrained to obey all the known applicable symmetry requirements and conservation rules. The resulting vertex functions may be related to coupling constants or form factors which one knows or can determine in principle from experiment. One also requires that all particles, external and internal, be placed upon the mass shell. Experimental values of masses, charges spins, vertex functions, and anomalous moments may thus be incorporated into a perturbation theory calculation in which the absorptive part of the amplitude is investigated.

In order to utilize the Mandelstam representation and accompanying formalism we must treat the deuteron as an "elementary" particle. We shall later explain our definition of "elementary" as compared to "composite."

In our treatment we neglect deuteron recoil. Because of the deuteron's large rest mass this is not a critical assumption. In the context of the theory, it involves approximating a very short branch cut by a pole.

Aside from these approximations the theory admits of more generality from the outset. The constraints which are applied to determine the analytic structure are the generalized Pauli principle, Lorentz and gauge invariance, invariance under spatial inversion, and unitarity. One very important result of this structure is the fact that one can separate and examine individually the roles of the various interactions and higher-order corrections such as meson exchange and final state nucleon rescattering. This possibility is developed from observations of the explicit influence of the cross channels in the scattering process. It will be seen that the exchange current contributions are inherently cross-channel effects. Indeed, it is just this property which impels us to imbed photodisintegration at threshold—an essentially nonrelativistic problem—into a relativistic framework. We expect mesonic effects to be relativistic. We hope to capitalize on the essential property of the Mandelstam representation which displays the relativistic character of the cross-channel effects.

The Details of the Calculation

For completeness, in Sec. 2, we summarize some of the results of SG, and provide definitions for the kinematical quantities appearing in the problem. We also discuss the reaction matrix which is linearly related to the S matrix and is composed of the sum of twelve invariant amplitudes defined by "vectors" spanning the transition space of spin and isospin. This space has dimensions defined by the internal degrees of freedom determined by the scattering process. In Sec. 3 we display the fixed-angle dispersion relations for the $M1$ dipole amplitude in terms of the relativistic invariant amplitudes.

The dispersion relation for the photomagnetic amplitude may be separated into three distinct terms. These are an integral over the left-hand (unphysical) cuts, the Born term, and an integral over the right-hand (physical) cut. In Sec. 4 we obtain the solution to this dispersion relation in several approximations.

On the right-hand cut we use an approximate form of unitarity to relate the real and imaginary parts of the amplitude. The phase shift in this relation is approximated using the effect range formula. The integral relations that result from this treatment of the right-hand cut are of the Omnes type.

The solutions are gained by following this procedure:

First, we exhibit the solution of the integral equation obtained by neglecting all contributions except those of the Born terms. This duplicates the results obtained in SG as well as some older nonrelativistic calculations.

Next, we parametrize the contributions made by all the left-hand singularities by condensing them into a δ function. The residue and position of this pole are fixed in functional form by a comparison with the experimental data.

Finally, we calculate the contributions made by the one-pion exchange current and final nucleon rescattering. These processes exhibit anomalous thresholds which determine branch cuts whose origins are much closer to the physical region than any other higher-order processes. The sum of the contributions from these cuts is approximated by another δ function which is compared with the one produced in the second step above. This direct comparison shows that addition of the exchange current contribution essentially eliminates the discrepancy between the experimental and the calculated cross sections.

Because the distances to singularities other than the one-pion exchange cut are quite large, the use of "polology", that is, the approximation of the cut structure by the condensation of its effects into poles, is a useful approximation in this low-energy application. Throughout this work we hold that local variation of the amplitude in the complex plane should be largely attributable to local singularities. Distant singularities may have a large absolute effect on the amplitude, but probably do not produce appreciable relative change in small regions distant from the singularity. We shall see that the important aspects of the integral representation are retained despite several nonrelativistic approximations. In the framework of the constraints we have outlined, we have used the increased facility in computation associated with pole approximations, combined with the clear indications of cross-channel effects, to affirm the cause for magnetic anomalies and resolve a discrepancy between theory and experiment.

There are several appendices which contain details supporting arguments in the main body of the paper.

2. KINEMATICS

Considering the deuteron as an ordinary spin-one elementary particle one may treat photodisintegration or the equivalent inverse process, $n-p$ capture, as one channel of the three scattering processes represented in Fig. 1.

Let k, d, p, and n be the four-momenta of the photon, deuteron, proton, and neutron, respectively. We define the scattering channels and the associated invariants as

$$\begin{array}{lll} \text{I} & \gamma+d\leftrightarrow p+n: & s=(k+d)^2=(p+n)^2 \\ \text{II} & d+\bar{n}\leftrightarrow \gamma+p: & t=(k-p)^2=(d-n)^2 \\ \text{III} & \gamma+\bar{n}\leftrightarrow \bar{d}+p: & u=(k-n)^2=(d-p)^2. \end{array} \quad (2.1)$$

Energy and momentum conservation require that

$$k+d=p+n. \quad (2.2)$$

Only three of these four momenta may be independent. The particle masses are introduced by requiring the four mass-shell constraints

$$k^2=0, \quad p^2=M^2, \quad d^2=D^2, \quad n^2=M^2. \quad (2.3)$$

(We use units $\hbar=c=m_\pi=1$. Scalar products are defined as $p_\mu p^\mu=p_0{}^2-\mathbf{p}^2$.) The invariants satisfy the relationship

$$s+t+u=2M^2+D^2=K. \quad (2.4)$$

The mass-shell constraint imposes the restriction that only two of the invariants s, t, or u may be taken as independent.

The three independent momenta will be taken as k, q, and Q. Here

$$Q=(p+n)/2, \quad q=(p-n)/2. \quad (2.5)$$

In the barycentric system we find for equal mass nucleons

$$Q=(E,0), \quad q=(0,\mathbf{p}). \quad (2.6)$$

The photon and deuteron polarizations are e_μ and U_ν. We impose the Lorentz and gauge conditions

$$\begin{array}{ll} e\cdot k=0, & e\cdot e=-1, \\ U\cdot d=0, & U\cdot U=-1. \end{array} \quad (2.7)$$

In terms of the center-of-mass (c.m.) three-momenta $\mathbf{k}$ and $\mathbf{p}$, and scattering angle θ defined by $\mathbf{k}\cdot\mathbf{p}=kp\cos\theta$, the invariants s, t, and u become

$$\begin{aligned} s&=4(M^2+p^2), \\ t&=M^2-2kE[1-(p/E)\cos\theta], \\ u&=M^2-2kE[1+(p/E)\cos\theta], \end{aligned} \quad (2.8)$$

where $E=(M^2+p^2)^{1/2}$. We construct the scalars

$$\nu=k\cdot Q/M, \quad \xi=k\cdot q/M. \quad (2.9)$$

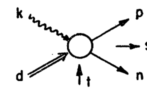

FIG. 1. Deuteron photodisintegration or the inverse process n-p capture.

From Eqs. (2.6) and (2.8) we find

$$\nu=(s-D^2)/4M, \quad \xi=(u-t)/4M. \quad (2.10)$$

We take $D=2M-B$, where B is the deuteron binding energy. Let $D^2\simeq 4(M^2-\gamma^2)$, where $\gamma^2=MB$. Thus

$$\nu\approx(p^2+\gamma^2)/M. \quad (2.11)$$

3. THE DISPERSION RELATIONS

Location of the Physical Region and Singularities

For photodisintegration or $n-p$ capture, the transition matrix is defined as

$$\begin{aligned} &\langle p,r;n,r'|T|k,e;d,U\rangle \\ &=(2\pi)^4\delta^4(n+p-k-d)[M^2/(2\pi)^{12}2\omega 2DE_pE_n]^{1/2} \\ &\quad\times\bar{w}_\alpha(\mathbf{p})\bar{w}_{\beta}{}^{r'}(\mathbf{n})M_{\alpha\beta}{}^{\mu\nu}(p,n;k,d)e_\mu(\mathbf{k})U_\nu(\mathbf{d}), \end{aligned} \quad (3.1)$$

where ω and D are the initial photon and deuteron energies, E_p and E_n are the energies of the final nucleons, $w_\alpha{}^r(\mathbf{p})$ is a spinor satisfying the Dirac equation and is normalized

$$\bar{w}^r(\mathbf{p})w^{r'}(\mathbf{p})=\delta_{rr'}. \quad (3.2)$$

It is convenient to reorder the spinors so that we may consider the matrix element taken between them. We may accomplish this by treating one of the outgoing nucleons as an incoming antinucleon. The reordered T matrix may be written as (apart from the δ function and constants)

$$\langle|T|\rangle\sim\bar{w}_\alpha{}^r(\mathbf{p})M_{\alpha\beta}{}^{\mu\nu}(p,n;k,d)\mathcal{C}_{\beta\beta'}\bar{w}_{\beta'}{}^{r'}e_\mu(\mathbf{k})U(\mathbf{d}). \quad (3.3)$$

Here we have

$$\mathcal{C}=i\tau_2 C, \quad (3.4)$$

where C is the charge conjugation Dirac matrix.

Apart from Lorentz covariance, the transition matrix elements are subject to the restrictions of the generalized Pauli principle, gauge invariance, and invariance under space inversion. For a given charge state, the Lorentz and gauge conditions on the polarizations, the requirement that the spinors satisfy the Dirac equation and the restrictions cited above determine the number of possible transitions which may occur from a given value of orbital momentum. There are twelve such transitions in this problem. Thus there are twelve independent covariant forms which describe the transition. Following SG we write

$$M_{\alpha\beta}{}^{\mu\nu}=\sum_{i=1}^{12} I_{\alpha\beta}{}^{\mu\nu}(i)H_i(\nu,\xi). \quad (3.5)$$

Here the H_i are scalar functions of the variables ν and ξ. The covariant forms which are listed in Table I in SG are constructed from the independent vectors q^μ,

Q^μ, k^{12}, and γ matrices. Note that Table I in SG is presented in the form $I^{\mu\nu}e_\mu U_\nu$. In the above, α and β are isotopic indices.

We may consider the twelve independent covariant forms of $I^{\mu\nu}$ as vectors in a particular separable Hilbert space. As we have seen, the dimensions in this transition space are determined by the internal degrees of freedom of the scattering process. It is useful to note that an orthonormal base for this space may be found. If we examine the SPAVT character of the covariant forms, we see that I_{12} is the only pseudovector form. We define scalar products as

$$I_i\cdot I_j=\tfrac{1}{4}\,\mathrm{Tr}[I_i^\dagger\cdot I_j]. \quad (3.6)$$

Thus I_{12} is orthogonal to all the other forms; since

$$I_{12}\cdot I_j=0 \quad \text{for all} \quad j\neq 0, \quad (3.7)$$

the transition matrix is linearly related to the scattering matrix. In our usage, $S=1+2iT$. We wish to exploit the unitarity of the S matrix and its particular implications in the photodisintegration process, namely, that the phase of the production amplitude in a single partial wave is the same as the scattering phase shift of the two-nucleon final state.

To apply unitarity it is necessary to relate the relativistically invariant amplitudes, $H_i(\nu,\xi)$, to the partial wave eigenamplitudes. This is accomplished in two steps. First, reduce the relativistic amplitudes to nonrelativistic amplitudes by writing the matrix elements in terms of Pauli instead of Dirac spinors. Then establish the relations connecting the nonrelativistic amplitudes to the dipole amplitudes by transforming the matrix element from its linear momentum representation to its equivalent angular momentum representation. The two sets of linear equations relating the eigenamplitudes to the relativistically invariant amplitudes have been formulated and solved in SG. These solutions are obtained for $\xi=$constant, and are simplest for $\xi=0$.

An alternative procedure to the SG for establishing the connections between the H_i and the dipole amplitudes has been provided by Bellac *et al.*[6] They relate the relativistically invariant amplitudes to the helicity amplitudes, which are then related to the multipole amplitudes.

In deuteron photodisintegration, the dominant process at threshold is the magnetic dipole spin-flip transition[7–9]

$$^3S_1+{}^3D_1\rightarrow {}^1S_0+{}^1D_2. \quad (3.8)$$

The D-state contribution is proportional to the square of the center-of-mass momentum, and thus the transition to the $^1D_2$ state is negligible in the threshold region. We may approximate the transition with an S wave and

[7] J. Blatt and V. Weisskopf, *Theoretical Nuclear Physics* (John Wiley & Sons, Inc., New York, 1952).

[8] J. S. Levinger, *Nuclear Photodisintegration* (Oxford Library of Physical Science, Oxford University Press, New York, 1960).

[9] H. Bethe and P. Morrison, *Elementary Nuclear Theory* (John Wiley & Sons, Inc., New York, 1956).

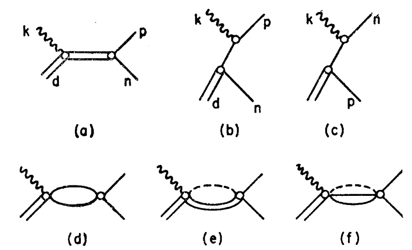

FIG. 2. Feynman diagrams of processes contributing the nearest singularities to $n+p\leftrightarrow\gamma+d$ at threshold. Wavy lines are photons, solid single lines nucleons, solid double lines deuterons, and dashed lines pions.

utilize the result that the transition amplitude is then independent of angle. This result enables us to write a fixed-angle dispersion relation for the amplitude. The correct choice of scattering angle allows simplification of the calculation.

We set $\xi=0$. This implies that $\mathbf{k}\cdot\mathbf{p}=0$, which in turn specifies scattering at 90° in the barycentric system. It will be shown that the physical region for channel I and the Mandelstam spectral functions are symmetric about the line $\xi=0$ in the $\xi\nu$ plane.

The magnetic dipole spin-flip amplitude designated as $M_1(^1S_0)$ may be found from Eqs. (2.15) and (2.16) in SG. We write

$$M_1(^1S_0)=\frac{1}{16\pi}\frac{\omega}{E}\left(H_{12}+\frac{2}{3}\frac{p^2}{M^2}H_{11}\right)_{\xi=0}. \quad (3.9)$$

Here, ω is the photon energy, E and p are the nucleon energy and momentum in the c.m. system. At threshold in the limit $p\rightarrow 0$ we have

$$M_1(^1S_0)=\frac{1}{16\pi}\frac{\omega}{E}[H_{12}]_{\xi=0}. \quad (3.10)$$

To write meaningful integral relations for the invariant amplitudes, we must assume that the H_j's are analytic functions of the variables ξ and ν except for isolated cuts and poles on the axis defined by $\xi=0$. We also assume that for fixed ξ

$$\lim_{\nu\rightarrow\infty} H_j\rightarrow 0 \quad \text{for all } j. \quad (3.11)$$

We may then apply the Cauchy theorem to write

$$\mathrm{Re}H(\xi,\nu)=\frac{1}{\pi}P\int_{-\infty}^{\infty}\frac{\mathrm{Im}H(\xi,\nu')d\nu'}{\nu'-\nu}. \quad (3.12)$$

Here, $P\int$ denotes the principal value of the integral. The path of integration will be defined when we have located the relevant singularities. This may be accomplished by examining the appropriate low-order graphs of the photodisintegration process. Some of these are shown in Figs. 2 and 3.

Mandelstam[10] has conjectured that *all* the diagrams associated with four leg processes like the one shown in Fig. 1 may be represented as analytic functions with

[10] S. Mandelstam, Phys. Rev. **112**, 1344 (1958).

poles corresponding to single-particle propagators and branch cuts describing multiparticle intermediate states. The amplitudes represented must be analytic in both energy and momentum transfer simultaneously.

In order to have all the poles appear explicitly in the dispersion relation, SG used a dispersion relation in the energy variable at a fixed difference of momentum transfer. This dispersion relation is equally valid as a fixed-momentum-transfer dispersion relation if the Mandelstam representation for this process is valid.

To utilize Eq. (3.12) in the context of the Mandelstam representation, we must locate the branch points and poles on the axis $\xi=0$ and thus define the regions where ImH exists. There are three such regions. They are the left-hand or unphysical cut, the Born poles, and the right-hand or physical cut.

The Physical Region

In general the physical region for a scattering process is defined in terms of the s, t, and u variables, so that the total energy in the center-of-mass system for a particular channel is greater than some threshold value, and the scattering angle is real. The details are clear when s, t, and u are depicted on a two-dimensional plot. The general prescription for constructing such a plot has been given by Kibble.[11]

A summary statement of the requirement for a real scattering angle may be put in the form of a homogeneous inequality in s, t, and u:

$$stu>(s+t+u)^2(as+bt+cu)\,, \tag{3.13}$$

where a, b, and c are defined in the relations

$$\begin{aligned} K^3a&=(2M^2-D^2)M^4\,,\\ K^3b&=M^2D^4\,,\\ K^3c&=M^2D^4\,,\\ K&=s+t+u=2M^2+D^2\,. \end{aligned} \tag{3.14}$$

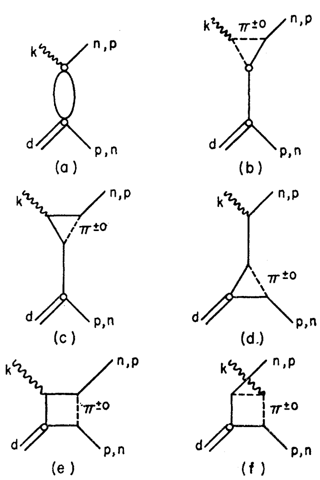

FIG. 3. Feynman diagrams of processes contributing the nearest singularities of the left-hand cut.

[11] T. W. B. Kibble, Phys. Rev. **117**, 1159 (1960).

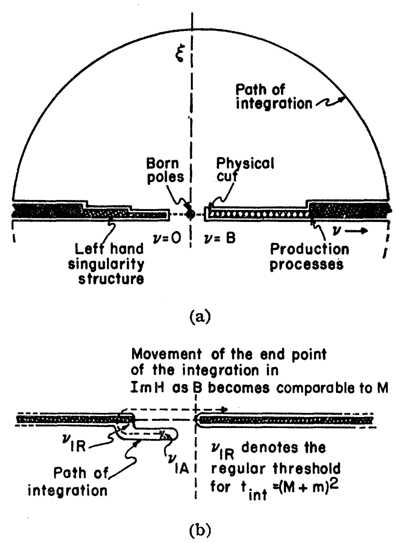

FIG. 4. (a) Singularity structure of the ξ, ν plane. (b) Migration of the anomalous part of the left-hand cut.

We may write Eq. (3.13) in terms of ξ and s as

$$4M^2\xi^2-f(s)<0\,, \tag{3.15}$$

where

$$f(s)=\tfrac{1}{4}s^2-\tfrac{1}{2}sK+K^2(\tfrac{1}{4}+b-a)-(K^3b/s)\,. \tag{3.16}$$

The energy inequalities are determined from the lowest-mass intermediate states appearing in channel I. These states are shown in Figs. 2(d)–(f). The lowest threshold is associated with the diagram in Fig. 2(d). In this instance

$$S\geq 4M^2 \quad\text{or}\quad \nu\geq B\,. \tag{3.17}$$

From Eq. (3.15) we find

$$|\xi|<[f(s)/2M]^{1/2}\,. \tag{3.18}$$

As s becomes large, the leading term in $f(s)$ of $O(s^2)$ dominates, and we find

$$\xi_{\text{asymp}}>s/4M\,. \tag{3.19}$$

Higher mass intermediate states, such as those accompanying production of additional particles, induce additional singularity structure at higher values of the energy variable. Some of this structure is indicated in Fig. 4(a). The boundaries of the physical region may be calculated using Eq. (3.16) and are shown in Fig. 7.

The cuts for the processes shown in Figs. 2(e) and 2(f) begin far to the right of thrshold and occur at a value of $s=(m+2M)^2$ or $\nu=145$ MeV. Here we have taken m as the pion mass. This is almost 75 times the distance to the Born poles and five times the distance to the singularities in the left-hand cut. Consistent with the hypothesis that in any local region of the ξ, ν plane only the nearest singularities affect variation, we neglect the cuts from higher mass processes.

The limits of integration over the right-hand cut are $B<\nu<\infty$. To set the limits on the left-hand cuts we must examine the thresholds of the diagrams representing the crossed t and u cuts. These are shown in Fig. 3.

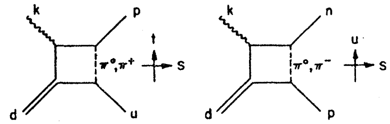

FIG. 5. The rescattering diagrams.

Figure 3(a) denotes the next lowest-mass intermediate states in channel II. This graph may be expanded into the vertex graphs seen in Figs. 3(b)–3(d) and the Landau diagrams seen in Figs. 3(e) and 3(f). These diagrams represent the left-hand singularity structure whose branch points are closest to the physical region. Figures 3(b) and 3(c) represent exchange and nucleon current contributions to the nucleon electromagnetic vertex. Figure 3(d) represents the deuteron structure due to the long-range part of the n-p potential, and indicates some of the properties of the d-np vertex. These three diagrams may not be considered regular Landau diagrams because the intermediate states indicated by 1 and 2 cannot both be the mass shell.[12] As shown, these are vertex diagrams and do not depend on s. The combination of diagrams indicated by Fig. 3(e) represents the structure of the final n-p state due to the long-range one-pion part of the n-p potential. We will refer to the two diagrams pictured in Fig. 3(e) as the rescattering diagrams. These diagrams are shown in more detail in Figs. 5(a) and 5(b). Figures 6(a) and 6(b) are the diagrams indicated by Fig. 3(f). These diagrams represent a part of the deuteron's structure due to mesonic exchange currents.

The Left-Hand Cuts. Anomalous Thresholds

The small size of the deuteron's binding energy compared to its rest mass produces anomalies in the thresholds in Landau diagrams in which the d-np vertex is a factor.

The threshold values of s, t, and u for the diagrams in Figs. 3(e) and 3(f) have been calculated by Alfaro and Rosetti[13] using the construction developed by Karplus *et al.*[14] They find that an anomalous threshold occurs for

$$t=u>M^2+2m^2+4m\gamma. \quad (3.20)$$

To find the branch point of the left-hand cuts on the axis $\xi=0$, we use the invariant sum cited in Eq. (2.4). The value of s corresponding to the values of t and u given in Eq. (3.20) is

$$s_{1A}=-4\gamma(\gamma+2m). \quad (3.21)$$

This point should not be confused with the regular threshold in s which is $s>4M^2$. In terms of the variable ν this becomes

$$\nu_{1A}=-m(m+2\gamma)/M. \quad (3.22)$$

This is the left-hand branch point nearest to the physical region. The notation is meant to indicate the single pion exchanged and the anomaly. A qualitative representation of the cut ν-plane is given in Fig. 4(a). The contributions of Figs. 3(b)–3(d) to the discontinuity structure of the left-hand cuts will be discussed at a later stage of this paper.

Anomalous thresholds appear in a dispersion-theoretical formalism when, because of certain mass ratios of participating particles, a cut migrates from the second sheet to the first, or when it becomes necessary to continue an amplitude from the first sheet to the second. The former view is more meaningful in our calculation.

One can actually follow the end point of the integration in ImH as it moves subject to a variation in the masses. Since this end point is a branch point in ImH, the path of the line integral in Eq. (3.12) must be deformed to avoid it. Stated another way, we may deform the line integral's path at will as long as we cross no branch points in the integrand ImH. Starting at a point where the deuteron binding energy is enough to give a "regular" threshold (albeit on the second sheet), we deform the path in such a way so that, when we decrease binding and the branch point moves, it will not cross the path of integration.

With either technique we produce the path shown in Fig. 4(b). The dotted line is the path of the branch point starting from its anomalous position and receding back to the second sheet as binding is increased.

If we neglect the cuts associated with higher-order processes, we see that the line integral over the left-hand cuts on the line $\xi=0$ is defined for $-\infty<\nu<\nu_{1A}$.

As an example of the formalism and to establish a scale for comparing the locations of the branch points associated with higher mass intermediate states, we calculate the threshold of a process in which a particle more massive than the pion is exchanged. A simple choice for the mass of this fictitious particle might be just double the pion mass. Inclusion of this mass value in the fourth-order exchange or rescattering diagrams [Figs. 3(e) and 3(f)] leads to the anomalous threshold values

$$t=u>M^2+8m^2+8m\gamma. \quad (3.23)$$

The point on the axis $\xi=0$ defined by this threshold is designated as ν_{2A} and is shown in Fig. 7. Reference to this double pion mass singularity will show that branch points corresponding to exchange of anything as massive as, for example, a ρ meson are very far from the secton of the physical region being studied.

The Born Poles

We have described the singularity structure associated with the multiparticle intermediate states. The

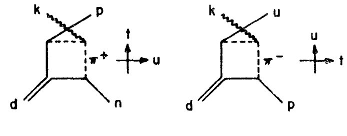

FIG. 6. The exchange diagrams.

[12] J. L. Morrison (private communication).

[13] V. Alfaro and C. Rossetti, Nuovo Cimento 18, 783 (1960).

[14] R. Karplus, C. M. Sommerfield, and E. H. Wichmann, Phys. Rev. 111, 1187 (1958).

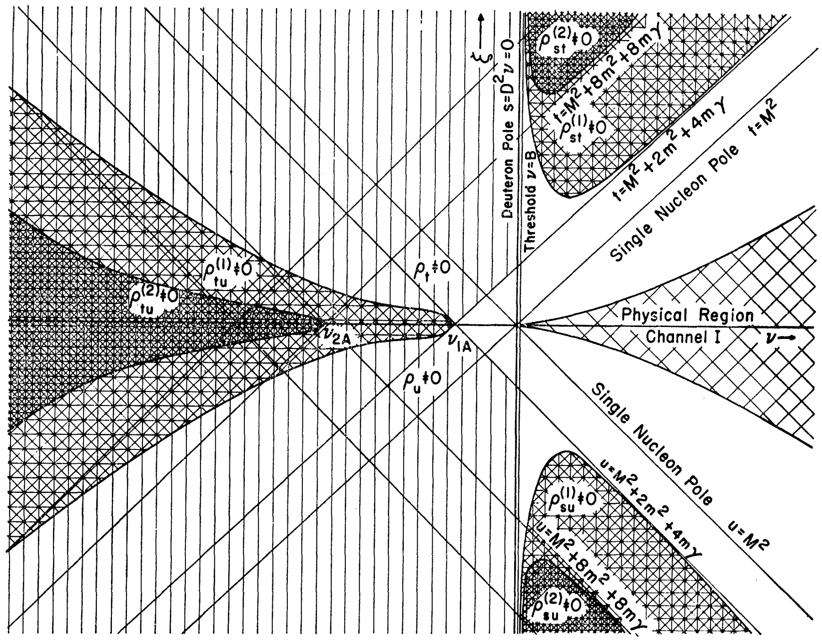

FIG. 7. Spectral functions and the physical region of channel I.

remainder of this structure—the single-particle intermediate states or Born poles—must now be discussed. These are represented by the diagrams shown in Figs. 2(a)–2(c). The poles associated with these diagrams have the forms $\rho_s/s-D^2$, $\rho_t/t-M^2$, and $\rho_u/u-M^2$. The quantities ρ_s, ρ_t, and ρ_u which are the residues of these poles may be calculated explicitly.[4,15,16] In SG it is shown that the residue of the pole in s, derived from the intermediate deuteron state [Fig. 2(a)], is proportional to $[\mu_p+\mu_n-(D/2M)\mu_d]$. Here, μ_p, μ_n, and μ_d are the nucleon and deuteron magnetic moments. The deuteron intermediate state requires a spin triplet, isoscalar final state. The poles in t and u associated with the intermediate nucleon states [Figs. 2(b) and 2(c)] have residues corresponding to both spin triplet isoscalar and to spin singlet isovector states. The isovector residues are proportional to $(\mu_p-\mu_n)$.

We neglect the D-wave amplitudes, since they are proportional to p^2 and are negligible at threshold.[17,18] Comparing the factors of proportionality, we see that the isovector ($^1S_0$) Born term is approximately a factor of 500 larger than the isoscalar ($^3S_1$) term. These poles are the closest singularities to the threshold of the physical region. This proximity makes them the dominant factors in determining the amplitudes in this region. This fact strengthens our earlier statement about the dominance of the $M_1(^1S_0)$ amplitude.

Incorporating the details of the cuts and poles, the integral in Eq. (3.12) may be written in terms of the ξ, ν variables as

$$\mathrm{Re}H(\nu)=\frac{1}{\pi}P\int_{-\infty}^{\nu_{1A}}\frac{\mathrm{Im}H(\nu')d\nu'}{\nu'-\nu}+\frac{\rho_t}{\nu+\xi}+\frac{\rho_u}{\nu-\xi}+\frac{1}{\pi}P\int_{B}^{\infty}\frac{\mathrm{Im}H(\nu')d\nu'}{\nu'-\nu}. \quad (3.24)$$

The Dispersion Relation for the $M_1(^1S_0)$ Amplitude

Following SG, we may transform the integral equation in Eq. (3.24) to our relating the real and imaginary parts of the $M_1(^1S_0)$ amplitude.

From Eq. (2.11) we see $\nu\simeq\omega$. We may rewrite Eq. (3.10) to read

$$M_1(^1S_0)=(\nu/16\pi M)H_{12}, \quad (3.25)$$

since at threshold we may disregard the dependence of E on ν. For convenience we represent the $M_1(^1S_0)$ amplitude as A.

The proportionality of A to ν requires that one modify the Cauchy integral formula to construct dispersion relations for A, or else that one write a dispersion relation for $\mathcal{A}$ where $A=\nu\mathcal{A}$.

If $A(\nu)$ is analytic at the point $\nu=0$, then we may apply the Cauchy formula to the function $[A(\nu)-A(0)]/\nu$. The dispersion relation takes the form

$$\mathrm{Re}A(\nu)=\mathrm{Re}A(0)+\frac{\nu}{\pi}P\int\frac{\mathrm{Im}A(\nu')d\nu'}{\nu'(\nu'-\nu)}. \quad (3.26)$$

---

[15] L. Durand III, Phys. Rev. **123**, 1393 (1961).

[16] R. Blankenbecler, M. L. Goldberger, and F. R. Halpern, Nucl. Phys. **12**, 629 (1959); M. L. Goldberger, Y. Nambu, and R. Oehme, Ann. Phys. **2**, 226 (1959); R. Blankenbecler and L. F. Cook, Phys. Rev. **119**, 1745 (1960).

[17] This point should not be construed as neglect of the percentage D-state of the deuteron. Although the D-wave transitions are negligible, there is a reduction of the initial $^3S_1$ wave function when the $^3D_1$ state is included in the description of the deuteron (Ref. 18). The deuteron description used in this calculation is obtained by matching the ratio of the asymptotic D and S wave functions to the deuteron quadrapole moment (Ref. 19).

[18] H. P. Noyes (private communication).

We may identify $\mathrm{Re}A(0)$ with the residues of the Born poles taken at $\xi=\nu=0f^{4-6}$

$$\mathrm{Re}A(0)=e(\mu_p-\mu_n)\Gamma[1-2\Delta(1+p^2/\gamma^2)], \quad (3.27)$$

where

$$\Gamma=\left[\frac{8\pi(\gamma/M)}{(1+2\Delta^2)(1-r_t\gamma)}\right]^{1/2} \quad (3.28)$$

and

$$\Delta=(1/\sqrt{2})\tan\epsilon|_{p^2=-\gamma^2}\simeq(1-r_t\gamma)Q\gamma^2. \quad (3.29)$$

Here r_t is the triplet effective range, Q is the deuteron quadrapole moment, and $\tan\epsilon$ is the Blatt and Biedenharn[19] parametrization of the ratio of the asymptotic scattering wave functions ^3D to ^3S. We shall neglect terms in $\mathrm{Re}A(0)$ which are proportional to Δ and to p^2. Let

$$b=e(\mu_p-\mu_n)\Gamma. \quad (3.30)$$

There is one additional argument we wish to introduce to form the dispersion relation. By unitarity the phase of the $M_1(^1S_0)$ amplitude from the onset of the physical cut to the point where higher mass channels are opened is the phase shift of the $^1S_0$ n-p scattering state. In the region $B<\nu\lesssim 140$ MeV we may state

$$\mathrm{Im}A(\nu)=\mathrm{Re}A(\nu)\tan\delta(\nu). \quad (3.31)$$

The contribution to the dispersion relation from the singularities associated with the opening of the higher mass channels should be negligible in the threshold region. We use the relation stated in Eq. (3.31) everywhere on the right-hand cut. Using Eqs. (3.30) and (3.31) we may rewrite Eq. (3.26) as

$$\mathrm{Re}A(\nu)=b+\frac{\nu}{\pi}\int_{-\infty}^{\nu_{1A}}\frac{\mathrm{Im}A(\nu')d\nu'}{\nu'(\nu'-\nu)} +\frac{\nu}{\pi}\int_{B}^{\infty}\frac{\mathrm{Re}A(\nu')\tan\delta(\nu')d\nu'}{\nu'(\nu'-\nu)}. \quad (3.32)$$

The solutions of this equation for several approximations are provided in Sec. 4.

4. SOLUTION OF THE DISPERSION RELATION

We shall provide separate solutions to Eq. (3.32) using three approximations. The first and most simple solution results from solving the equation neglecting the left-hand cuts. This procedure yields the Born amplitude. This amplitude yields a cross section some 5% lower than the experimental cross section obtained for thermal neutron capture.

In the next step we condense the left-hand singularities into a single pole. The dispersion relation is solved using this pole as additional input. The residue and position of this additional pole are adjusted so that the resulting cross section agrees with the experimental value.

[19] L. Biedenharn and J. Blatt, Phys. Rev. **93**, 1387 (1954).

Finally we calculate $\mathrm{Im}A$ in the region of the anomalous part of the left-hand cuts. We find that $\mathrm{Im}A$ which is essentially $[A(\nu+i\epsilon)-A(\nu-i\epsilon)]$—that is, the jump across the cut—is much larger in the region of the anomalous threshold than at more distant locations on the cut. Therefore, we fit the portion of the left-hand integral, whose limits are determined by the anomalous part of the cut, to another pole. The parameters of this pole are found to agree very nearly with their analogs associated with the "phenomenological" ploe mentioned above. This agreement indicates that inclusion of some of the left-hand singularity structure does yield a cross section in closer agreement with experiment.

The Born Amplitude

The solution of equations like Eq. (3.32) without the left-hand integral has been developed by Omnes.[20] A statement of this method may be found in Appendix A. We shall provide an alternative treatment for the Born amplitude which is somewhat simpler and illustrates some of the analytic properties of the amplitude in the cut energy plane.

First, we suppose that the whole amplitude is described by the $^1S_0$ partial wave behavior, and is thus subject to a partial wave treatment. In this instance the N/D method can be very useful. Following Omnes,[20] define the denominator function $D(\nu)$ as

$$D(\nu)=\exp\left[-\frac{\nu}{\pi}\int_{B}^{\infty}\frac{\delta(\nu')d\nu'}{\nu'(\nu'-\nu)}\right], \quad (4.1)$$

which is normalized to unity at the Born pole, is real on the negative axis, cut along the positive axis for $B<\nu'<\infty$ where it has the phase $-\delta(\nu')$.

Define the numerator function $N(\nu)$ as

$$N(\nu)=D(\nu)A(\nu) \quad (4.2)$$

or

$$A(\nu)=N(\nu)/D(\nu). \quad (4.3)$$

From Eq. (4.3) one sees that $N(\nu)$ has the same left-hand cut properties as $A(\nu)$ but no right-hand cut.

Note that the magnetic dipole matrix element has the property that at $\nu=0$ then $A_{M1}=$ constant, since all $M1$ matrix elements contain a factor ν and only the Born term has a denominator which vanishes at $\nu=0$. With this as a guide, we observe that if we neglect the left-hand cuts and suppose the pole terms determine $N(\nu)$, we may write for behavior near threshold[21]

$$N(\nu)=N(0)=A(0)$$

or

$$D(\nu)A(\nu)=D(0)A(0)$$

$$A(\nu)=[D(0)/D(\nu)]A(0)=b[D(0)/D(\nu)]. \quad (4.4)$$

[20] R. Omnes, Nuovo Cimento **8**, 316 (1958).
[21] B. Bosco, Nuovo Cimento **26**, 342 (1962).

TABLE I. Effective range parameters (HS, Ref. 22).

Triplet	Singlet
$a_t=5.39\pm0.03$ F	$a_s-23.74\pm0.09$ F
$r_t=1.704\pm0.028$ F	r_s 2.67 ± 0.028 F
$\alpha_+>0$	$\alpha_+>0$
$\alpha_-<0$	$\alpha_->0$

This same result may be obtained using arguments provided by MacDowell[22] for a more general case.

We may exploit the approximate form of unitarity we have stated to obtain an analytic form for $D(\nu)$, and thus obtain an explicit solution for Eq. (4.4). We have identified the phase on the physical cut as that of the ${}^1S_0$ phase of the final nucleon system. We shall utilize the effective range approximation to provide an analytic form for the phase shift. This approximation should be very accurate at threshold.

The "rescattering" amplitude for S waves may be written as

$$A_0=e^{i\delta_0}\sin\delta_0/p=(p\cot\delta_0-ip)^{-1}, \tag{4.5}$$

and for S waves the effective range approximation has the form

$$p\cot\delta_0=-1/a+\tfrac{1}{2}rp^2+\cdots. \tag{4.6}$$

In the above, p is the c.m. momentum, δ_0 is the phase shift, a is the scattering length, and r is the pertinent (singlet or triplet) range. Using (4.5), the amplitude can be written

$$A_0=(\tfrac{1}{2}rp^2-ip-1/a)^{-1}. \tag{4.7}$$

Observe that the amplitude A_0 and $1/D$ have the same phase but not the same left-hand singularity structure. If we neglect all left-hand singularities except the Born poles, we may set $A=1/D$. One sees that the quadratic form of the denominator in Eq. (4.7) will yield two poles in the amplitude in the complex p plane, or one pole on one of the two sheets in the complex p^2 plane. Observe

$$A=2[r(p-i\alpha_+)(p-i\alpha_-)]^{-1}, \tag{4.8}$$

where

$$\alpha_\pm=\frac{1}{r}[(1-2r/a)^{1/2}\pm1]. \tag{4.9}$$

Table I lists the relevant triplet and singlet data from Hulthén and Sugawara[23] (henceforth referred to as HS) and the location of the poles in the p^2 plane.

TABLE II. Effective range parameters (Noyes, Ref. 23).

$a_t=5.396\pm0.011$ F;	$a_s=-23.678\pm0.028$ F;
$r_t=1.726\pm0.014$ F;	$r_s=2.51\pm0.11\pm0.0435$ F

[22] S. W. MacDowell, Phys. Rev. Letters **6**, 385 (1961).

[23] L. Hulthén and M. Sugawara, in *Handbuch der Physik*, edited by S. Flügge (Springer-Verlag, Berlin, 1957), Vol. 39, p. 129.

Noyes[24] has given another set of values for the effective range parameters which are supposedly more consistent for n-p scattering. They are calculated from the existing n-p scattering data below 20 MeV. These are cited in Table II. The second error quoted for r_s is a conservative estimate of the uncertainty due to departures from the shape-independent approximation.

From the values of $\alpha_\pm$ listed in Table I, we see that in the triplet case the pole is on the physical sheet of the p^2 plane. This is the deuteron pole corresponding to the bound state. For the singlet case, the pole is on the unphysical sheet near the onset of the physical branch cut. This corresponds to the deuteron virtual singlet state. Eden[25] has given a more detailed argument about the effective range poles in the content of the N/D formalism.

To complete the transition from effective range amplitude to denominator function, we manipulate the poles in the following way. Since $1/D$ has the same phase as A but not the same left-hand singularities, for each pole of A on the real energy sheet we replace the singularity but do not change the phase. For instance, if A has a pole at $p=ia$, replace $1/(p-ia)$ by $(p+ia)$, thus removing the singularity but keeping the phase the same.[26] Use this procedure and see that

$$\frac{1}{D(p)}=\frac{2}{r}\left(\frac{p+i\alpha_+}{p+i\alpha_-}\right). \tag{4.10}$$

It can be shown that substitution of

$$\delta=\cot^{-1}[-1/ap+\tfrac{1}{2}rp] \tag{4.11}$$

into Eq. (4.1) yields a $D(\nu)$ equivalent to that in Eq. (4.10).

We may now evaluate Eq. (4.4) as

$$A(p)=\left(\frac{p+i\alpha_+}{p+i\alpha_-}\right)\left(\frac{\gamma+\alpha_-}{\gamma+\alpha_+}\right)A(0). \tag{4.12}$$

Note $p=i\gamma$ at $\nu=0$.

If we write $A(p)$ in the form

$$A(p)=e^{i\delta(p)}A(0)\hat{A}(p), \tag{4.13}$$

we may manipulate the expression in Eq. (4.12), resue the effective range formula, and find

$$\hat{A}(p)=\frac{-\sin\delta(p)}{ap}\left[1-\gamma a-\tfrac{1}{2}rap^2+\frac{(p^2+\gamma^2)a}{(\gamma+\alpha_+)}-2\Delta p\frac{2(1-2r/a)^{1/2}}{\gamma^2 r}\right], \tag{4.14}$$

$$\hat{A}(p)\approx\frac{-\sin\delta(p)}{ap}\left[1-\gamma a-\tfrac{1}{2}rap^2+\frac{(p^2+\gamma^2)a}{(\gamma+\alpha_+)}\right].$$

[24] H. P. Noyes, Phys. Rev. **130**, 2025 (1963).

[25] R. J. Eden, *Brandeis Summer Lectures in Theoretical Physics* (W. A. Benjamin Company, New York, 1962).

[26] B. Sakita and C. Goebel (unpublished).

We have chosen $p=+i\gamma$ for consistency on the physical sheet. A solution identical to Eq. (4.14) is obtained by using the analytic form of the effective range phase shift in the integral equation.

Calculation of the Born Capture Cross Section

The total cross section for photomagnetic disintegration of the deuteron at threshold may be calculated using the amplitude as stated above; and following Eqs. (4.10) and (2.13) in SG we find

$$\sigma=\frac{2\pi}{3}\frac{1}{M^2}\left(\frac{e^2}{4\pi}\right)(\mu_p-\mu_n)^2\frac{p\gamma}{(1-r_t\gamma)(p^2+\gamma^2)}\hat{A}^2(p). \quad (4.15)$$

We have neglected terms proportional to the D state.

In the zero-range approximation where r_t and r_s approach zero, Eq. (4.15) reduces to

$$\sigma=\frac{2\pi}{3}\frac{1}{M^2}\left(\frac{e^2}{4\pi}\right)(\mu_p-\mu_n)^2\frac{p\gamma}{p^2+\gamma^2}\frac{(1-\gamma a_s)^2}{1+(pa_s)^2}. \quad (4.16)$$

The expression shows agreement with the standard result as derived, for instance, by Blatt and Weisskopf.[7]

To find the cross section for the inverse process of photodisintegration, namely, n-p capture, one utilizes the principle of detailed balance. Then

$$\sigma_{\text{cap}}=\frac{\pi}{M^2}\left(\frac{e^2}{4\pi}\right)(\mu_p-\mu_n)^2\left(\frac{\gamma}{M}\right)\frac{(p^2+\gamma^2)}{(1-r_t\gamma)(pM)}\hat{A}^2(p). \quad (4.17)$$

The "Born" capture cross section is the one computed using the form of $A(p)$ given in Eq. (4.14). The other constants used are

$$M=938\text{ MeV}=4.754\text{ F}^{-1},\qquad e^2/4\pi=1/137,$$
$$\gamma=45.68\text{ MeV}=0.2315\text{ F}^{-1},\quad (\mu_p-\mu_n)=4.706, \quad (4.18)$$

$\sigma_{\text{cap}}(\text{experimental})=0.3315\pm0.0017$ barns.[27,28]

The singlet and triplet ranges r_s and r_t have been cited in Tables I and II. In the above, we have taken $p=1.743\times10^8\text{ cm}^{-1}$, since for thermal neutrons the c.m. velocity is 1100 m/sec. The kinetic energy of nucleons associated with this value is much less than any other energetic quantity used. Thus the thermal cross section accurately describes threshold behavior.

Using a calculation of the thermal n-p capture cross section by Austern and Rost,[29] Noyes notes that use of the smaller value of the singlet range given in Table II in this cross section makes the discrepancy between the computed and observed value nearly disappear. This is not quite accurate.

[27] R. W. Stooksbury and M. F. Crouch, Phys. Rev. **114**, 1561 (1959).

[28] In a private communication, Noyes has mentioned a measurement of this cross section by S. Wychank. The value reported is $\sigma=0.3342\pm0.0005$ barns. This value increases the discrepancy between theory and experiment. We have based the remainder of our work on the value for the cross section stated in Eq. (4.18), since Wychank's result is unpublished.

[29] N. Austern and E. Rost, Phys. Rev. **117**, 1506 (1959).

Austern and Rost describe the capture process in terms of a "reduced", nonmesonic matrix element. They write

$$\mathfrak{M}=\frac{1-\gamma a_s}{-\gamma^2 a_s}-\frac{r_s+r_t}{4}\quad\text{(in fermis, F)}, \quad (4.19)$$

$$\mathfrak{M}=5.1056-1.0935=4.0121\text{ (using HS)},$$
$$\mathfrak{M}=5.1077-1.0590=4.0487\text{ (using Noyes)}, \quad (4.20)$$

$$\mathfrak{M}_{\text{Born}}=5.1056-0.9799=4.1258\text{ (using HS)},$$
$$\mathfrak{M}_{\text{Born}}=5.1077-0.9359=4.1718\text{ (using Noyes)}. \quad (4.21)$$

The experimental value is

$$\mathfrak{M}_{\text{Born}}=4.18. \quad (4.22)$$

The larger errors in the values for the effective ranges given by Noyes will not allow the conclusion that use of these phase parameters will eliminate the discrepancy between calculation and experiment. In the remainder of the calculation we shall use the HS parameters. The algebra will be complete enough so that anyone who wishes to check the results by injecting Noyes' parameters may do so.

Substituting the values in Eq. (4.18) into Eq. (4.17), we find the Born capture cross section is

$$\sigma_{\text{Born}}=0.323\text{ barns}. \quad (4.23)$$

Parametrization of the Remaining Left-Hand Structure

We shall show that the remainder of the left-hand singularity structure can be effectively condensed into a pole with an appropriately chosen location and residue. For both ν and $\nu_c\leq\nu_{1A}$, let

$$\operatorname{Im}A=-\pi R\delta[\nu-(\nu_c)]. \quad (4.24)$$

This approximation of the imaginary part of the amplitude yields a bounded integrand for the principal part of the left-hand integral. The dispersion relation becomes

$$A(\nu)=b\left[\frac{\bar{R}}{\nu+\nu_c}+d(p)\right]+\frac{\nu}{\pi}\int_B^\infty\frac{A(\nu')\tan\delta(\nu')d\nu'}{\nu'(\nu'-\nu-i\epsilon)}, \quad (4.25)$$

where

$$R=e(\mu_p-\mu_n)\Gamma\bar{R}=b\bar{R}, \quad (4.26)$$

and

$$d(p)=1-2\Delta(1+p^2/\gamma^2). \quad (4.27)$$

The details of the solution of Eq. (4.25) are given in Appendix A. In the following let

$$\frac{\bar{R}}{\nu+\nu_c}=\frac{\bar{R}M}{p^2+p_c^2+2\gamma^2}=\frac{\bar{R}M}{p^2+l_c^2}=r(p). \quad (4.28)$$

Upon changing to momentum variables, Eq. (4.25) becomes

$$A(p)=b[r(p)+d(p)]+\frac{p^2+\gamma^2}{\pi}\int_0^\infty \frac{A(q)\tan\delta(q)dq^2}{(q^2+\gamma^2)(q^2-p^2-i\epsilon)}. \quad (4.29)$$

From Appendix A one sees that the solution takes the form

$$A(p)=e^{1\delta(p)}b[r(p)+d(p)]\cos\delta(p)+e^{\tau(p)-\tau(\infty)}\times\cos\delta(\infty)2\Delta(1+p^2/\gamma^2)+\frac{p^2+\gamma^2}{\pi}[D(p)]^{-1}P\times\int_0^\infty\frac{[r(q)+d(q)]\sin\delta(q)D(q)dq^2}{(q^2+\gamma^2)(q^2-p^2)}. \quad (4.30)$$

Here

$$D(p)=e^{-\tau(p)}, \quad (4.31)$$

where $D(p)$ is the Omnes denominator function of Eq. (4.1) written in p^2

$$D(p)=\exp\left[-\frac{p^2+\gamma^2}{\pi}P\int_0^\infty\frac{dq^2\delta(q)}{q^2(q^2-p^2)}\right]. \quad (4.32)$$

The integrand in Eq. (4.30) is the sum of two parts—the Born part and that part coming from the new pole. We already have the part of the amplitude generated by the Born term. This was the amplitude given in Eq. (4.14). We refer to this amplitude as $A_0(p)$. We can thus rewrite Eq. (4.30) as

$$A(p)=e^{i\delta(p)}bA_0(p)+r(p)+\frac{2|\bar{R}|M}{r_s(\gamma^2-\alpha_+^2)}\left(\frac{p^2+\alpha_+^2}{p^2+\alpha_-^2}\right)^{1/2}\frac{p^2+\gamma^2}{l_c^2-\alpha_+^2}\,\frac{\alpha_+}{p^2+\alpha_+^2}+\frac{c^{(\gamma 2-\alpha+2)}}{(p_c^2+\gamma^2)(p^2+l_c^2)}-\frac{\gamma}{p_c^2+\gamma^2}. \quad (4.33)$$

To evaluate $\cos\delta(p)$, we used the Levinson theorem[21,30]

$$\delta(0)-\delta(\infty)=n\pi, \quad (4.34)$$

where n is the number of bound states created by the potential in the particular angular momentum state. We have made assumptions that require $\delta(\infty)=0$. Hence, $\delta(0)=0$. This is verified if one notes that the deuteron singlet state is virtually bound. Thus $\delta(0)=0$, $\cos\delta(0)\approx\cos\delta(p)=1$.

We write the experimental cross section as

$$\sigma_{\text{cap}}=c[A_{\text{cap}}(p)]^2. \quad (4.35)$$

Here

$$c=1.172\text{ F}^2;\quad A_{\text{cap}}^2=28.31. \quad (4.36)$$

[30] N. Levinson, Kgl. Danske Videnskab. Selskab, Mat. Fys. Medd. 25, 9 (1949).

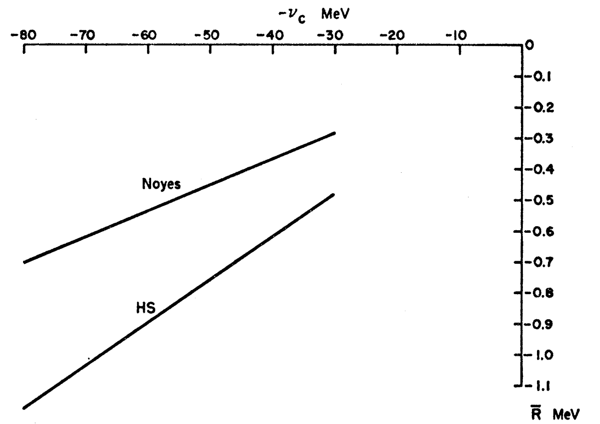

FIG. 8. Placement and residue of the pole to approximate the left-hand cut. The point indicated represents the pole properties calculated from the fourth-order exchange contribution.

We shall use the experimental value of the cross section to see what A_{pole} must be. Then we shall obtain a function of residue $\bar{R}$ versus position ν_c. This approach is the only one available because there is only one energy for which a value of the capture cross section has been obtained experimentally. It would be extremely useful if the cross section could be evaluated at another energy energy close to threshold. If this were the case, then the first pole's residue and position could be evaluated independently. In this instance use of the pole as a standard for comparison would be more meaningful. Until such experiments are performed we must rely on the single cross section datum.

We write the reduced matrix element as

$$A(p)=A_0(p)+A_{\text{pole}}(p). \quad (4.37)$$

We find

$$A_0^2=27.55\text{ (using HS)}. \quad (4.38)$$

From Eq. (4.33)

$$A_{\text{pole}}=\frac{\bar{R}M}{p^2+l_c^2}+\frac{2\bar{R}M}{r_s(\gamma^2-\alpha_+^2)}\left(\frac{p^2+\alpha_+^2}{p^2+\alpha_-^2}\right)^{1/2}\frac{p^2+\gamma^2}{l_c^2-\alpha_+^2}\times\frac{\alpha_+}{p^2+\alpha_+^2}+\frac{l_c(\gamma^2-\alpha_+^2)}{(p_c^2+\gamma^2)(p^2+l_c^2)}-\frac{\gamma}{p_c^2+\gamma^2}. \quad (4.39)$$

From Eq. (4.28) we see that $M\nu_c=p_c^2+\gamma^2$; $l_c^2=M\nu_c+\gamma^2$. Define

$$A_{\text{pole}}=-\bar{R}Ma(\nu_c). \quad (4.40)$$

Using Eq. (4.40) and letting $p^2\to 0$, we write

$$a(\nu_c)=\frac{1}{\nu_c+B}+K\left(\frac{\gamma^2}{\nu_c+L/M}\right)\alpha_+^{-1}+\frac{L/M}{\nu_c(M\nu_c+\gamma^2)^{1/2}}-\frac{\gamma}{\nu_c}, \quad (4.41)$$

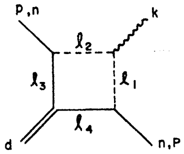

FIG. 9. The Feynman diagrams representing exchange corrections. We have here indicated exchange of final nucleons and the accompanying exchange of both charged mesons. For graphical simplicity we have uncrossed the photon and nucleon lines as they appeared in Figs. 7(a) and 7(b).

where

$$K=\frac{2}{r_sL}\left|\frac{\alpha_+}{\alpha_-}\right|;\quad L=\gamma^2-\alpha_+{}^2. \tag{4.42}$$

From our definition

$$\sigma=c[A_0{}^2-2\bar{R}Ma(\nu_c)A_0+\bar{R}^2M^2a^2(\nu_c)], \tag{4.43}$$

$$\bar{R}=\frac{A_0-[\sigma_{\rm exp}/c]^{1/2}}{Ma(\nu_c)}, \tag{4.44}$$

where the negative sign is chosen for the radical since the difference between $(\sigma_{\rm exp}/c)^{1/2}$ and A_0 is required. The consequence of this choice is that $\bar{R}<0$.

Figure 8 is a plot of $\bar{R}$ versus ν_c as calculated from Eq. (4.44) and the above. We have used both the HS and Noyes parameters in calculating $\bar{R}(\nu_c)$. In this calculation note that the Noyes pole is always weaker than the corresponding HS pole at the same location. One sees that it is the smaller value of the Noyes singlet range that induces this result.

Figure 8 exhibits the relation between the residue and the placement of the pole, which, when inserted into the calculation, improves agreement between the values of the calculated and experimental cross sections.

This phenomenological pole may be used to test the effects on the amplitude imposed by the higher order corrections.

To effect this comparison the additional contributions are cast in pole form. The departure from precision in this approximation is not great if we confine our efforts to short cuts which are quite distant from the region under investigation.

The parameters of the newly calculated pole are compared to their analogs associated with the phenomenological pole. If, at a given placement, the residues of the poles are widely different, we can see that injection of the new pole into the integral equation for the amplitude will not produce a result that leads to a cross section which will agree with the experimental value.

In the next section we will calculate those contributions to the amplitude which are produced by the foruth-order (in perturbation theory) meson exchange and final state rescattering processes [Figs. 3(e) and 3(f)]. We shall also examine the effects derived from contributions to the deuteron structure due to the long-range part of the n-p potential [Fig. 3(d)].

A More Exact Treatment of the Left-Hand Cut Structure

The pertinent Feynman amplitudes for photodisintegration have been described rather generally. We now wish to amplify some of these statements and examine in detail the fourth-order (box) diagrams which represent the exchange and rescattering corrections.

The exchange diagram is treated first, since it proves to be the more important in our region of interest. The methods used to treat exchange are then applied with minor changes to the rescattering correction.

The various external and internal four-momenta of the exchange diagram are labeled in Fig. 9.

First note that the character of the exchange diagrams is purely isovector. This is a consequence of the presence of the $\gamma\pi\pi$ vertex.[31] We have already noted that only the isovector contribution of the rescattering diagrams will enter.

The analytic properties of Feynman amplitudes have been studied in detail and the criteria for location of various singularities have been established.[32] We shall continue along lines suggested by Cutkosky[33] and Mandelstam[34] to find the discontinuity across the fourth-order exchange and rescattering cut beginning at the anomalous branch points. The singularities of the discontinuity functions may then be found and related to the appropriate spectral functions.

Heretofore, spectral functions have been computed using their topological properties and the mass ratios of member particles. Most workers have treated all particles as scalar in character. In this approach one utilizes the relations between the invariants (s, t, and u), the masses of the incoming and outgoing particles, and the mass shell properties of the internal propagators. Much can be learned from this alone. We have exhibited threshold placement cut structure, and the relative influence of the several higher-order corrections using the limits indicated by the "scalar" theory outlined above. If, however, we wish to obtain quantitative results, we must reconsider particle properties and account for spinor, pseudoscalar, etc., as well as kinematical factors.

This presents an additional difficulty. In the scalar case we sought to find the Lorentz invariants which described the scattering process and were free of kinematical singularities. When all spins are accounted for, we still hope to find invariant amplitudes with the same dynamical singularity structure exhibited in the scalar case. A procedure for generating these invariants, free of kinematical singularities, has been proposed by Hearn[35] for all processes except those involving one

[31] W. R. Frazer, *Electromagnetic Structure of the Pions and Nucleons*, Scottish Universities Summer School 1960, edited by G. R. Screaton (Interscience Publishers, Inc., New York, 1961).
[32] L. D. Landau, Nucl. Phys. **13**, 181 (1959).
[33] R. E. Cutkosky, J. Math. Phys. **1**, 429 (1960).
[34] S. Mandelstam, Phys. Rev. **115**, 1742 (1959).
[35] A. C. Hearn, Nuovo Cimento **21**, 333 (1961).

photon. We have found that in these one-photon processes the use of gauge invariance to construct the invariants invariably leads to the injection of kinematical singularities in some of them. Yet, these selfsame gauge requirements can be used to calculate the residues of the injected singularities. One may then follow a subtraction procedure enunciated by Ball[36] to remove these effects.[37] O'Donnell[38] has shown that the covariant forms provided by SG are superior to those provided by Donnachie[5] since the former do not contain "unnecessary" singularities. In any case we note that there are no kinematical singularities generated in the construction of $I_{12}^{\mu\nu}$.

The complete Feynman amplitude is obtained by summing the contributions from both exchange diagrams implied by Fig. 9. Using Schweber's[39] rubric for displaying the various factors, we find

$$F_4=\delta(n+p-k-d)\left[\frac{M^2}{(2\pi)^{12}2\omega 2DE_pE_n}\right]^{1/2}8G^2eM \times\int\frac{d^4N}{\prod_i(l_i^2-m_i^2)}. \quad (4.45)$$

Here

$$N=\bar{w}(p)\epsilon_\mu(l_1^\mu+l_2^\mu)\gamma_5(\boldsymbol{l}_3+M) \times\left[-\tilde{F}\boldsymbol{U}+\frac{\tilde{G}}{M}(l_3\cdot U)\right]\gamma_5(\boldsymbol{l}_4+M)w^C(n)$$

$$\prod_i(l_i^2-m_i^2) =(l_1^2-m^2)(l_2^2-m^2)(l_3^2-M^2)(l_4^2-M^2). \quad (4.46)$$

The quantities $\tilde{F}$ and $\tilde{G}$ are defined as

$$\tilde{F}=-\left[\frac{8\pi(\gamma/M)}{(1+2\Delta^2)(1-r_t\gamma)}\right]^{1/2} \quad (4.47)$$

$$\tilde{F}=3(M^2/\gamma^2)\Delta\Gamma. \quad (4.48)$$

The details of the *d-np* vertex used above are provided by Durand[15] and Blankenbecler[16] and elaborated by SG. In this vertex we have assumed we could replace the outgoing nucleons with the mass shell nucleon propagators, and that the proper normalization could be provided. Thus one finds that the *d-np* vertex part of the fourth-order diagram contributes a factor

$$[1/(2\pi)^3 2D]^{1/2}[-\gamma_\nu 2M\tilde{F}+l_{3\nu}\tilde{G}]U^\nu. \quad (4.49)$$

We have neglected the "relativistic" invariants in the *d-np* vertex description. This is a reasonable approximation at the threshold energies we are considering. However, there are indications that these invariants should be retained in calculations where the energy is above threshold but not necessarily in the relativistic region.[40]

Let us separate the common factors of the R matrix from the rest and write

$$F_4=R_{<>}\frac{8G^2eM}{(2\pi)^4}\int\frac{d^4N}{\prod_i(l_i^2-m_i^2)} \quad (4.50)$$

$$R_{<>}=(2\pi)^4\delta(n+p-k-d)\left[\frac{M^2}{(2\pi)^{12}2\omega 2DE_pE_n}\right]^{1/2}. \quad (4.51)$$

We have seen that each T-matrix element may be represented as a 12-fold sum of Lorentz covariants multiplied by the invariant amplitudes. The quantity N defined in Eq. (4.46) contains this summed structure intrinsically. Cutkosky has shown that the integral in Eq. (4.50) gives the discontinuity function from which the Mandelstam spectral functions are obtained. The discontinuities of this function occur when all the $(l_i^2-m_i^2)$ vanish.[33,34] These properties, derived from the common denominator, are juxtaposed onto all the invariants appearing in the amplitude. We must therefore find a way to discriminate in N and select those elements of the polynomial which correspond to the amplitude for which we are writing dispersion relations. Recall that this is the amplitude associated with the invariant I_{12} for the photomagnetic disintegration process at threshold. Using Eqs. (3.6) and (3.7), we may find the amplitude by evaluating the quantity

$$C=I_{12}\cdot N/|I_{12}|^2 \quad (4.52)$$

on the mass shell. The details of this procedure are provided in Appendix B. We find that

$$C=-2m^2M\Gamma(L+\Delta). \quad (4.53)$$

We shall henceforth neglect Δ.

We have operated on a vector sum in the integrand and projected out the coefficient of a particular vector in which we are interested. Examination of Eq. (4.53) indicates that this expression involves no kinematical factors when evaluated on the mass shell, and thus may be taken outside the integral.

If one constructs the second-order Born amplitudes using the *d-np* vertex as cited above and employs the same projection technique, the residues which are obtained agree with those obtained by SG.

To relate the amplitude given in Eq. (4.50) to the one for which we write dispersion relations, we inject the factor $(16\pi)^{-1}$ consistent with Eq. (3.25). The amplitude now takes the form

$$A_4=-R_{<>}\frac{G^2eM^2m^2\Gamma}{(2\pi)^4\pi}\int\frac{d^4l}{\prod(l_i^2-m_i^2)}. \quad (4.54)$$

The discontinuity in this function which occurs when all the factors $(l_i^2-m_i^2)$ vanish may be computed by taking

[36] J. Ball, Phys. Rev. **124**, 2014 (1961).
[37] J. Morrison (private communication).
[38] P. O'Donnell (private communication).
[39] S. Schweber, *An Introduction to Relativistic Field Theory* (Row, Peterson, and Company, Elmsford, New York, 1961).

[40] F. Gross, Phys. Rev. **134**, B405 (1964).

the difference when each mass has a small positive, then a small negative, imaginary part. This is equivalent to replacing $[l_i^2-m_i^2]$ by $i\pi\delta(l_i^2-m_i^2)$. The discontinuity of the discontinuity function is written as

$$A_4=-\frac{R_{<>}G^2eM^2m^2\Gamma}{16\pi}\int d^4l\delta(l_1^2-m^2)\times\delta(l_2^2-m^2)\delta(l_3^2-M^2)\delta(l_4^2-M^2). \quad (4.55)$$

In the scalar case, the Mandelstam spectral function is, apart from a factor of $\frac{1}{4}$, given by

$$\int d^4l\delta(l_1^2-m^2)\cdots. \quad (4.56)$$

Mandelstam's result can be obtained using Cutkosky's transformation

$$d^4l\rightarrow dl_1^2dl_2^2dl_3^2dl_4^2. \quad (4.57)$$

The Jacobian of this transformation is

$$J=\det(\partial l_i^2/\partial l_\mu)=2^4\det l_{i\mu}. \quad (4.58)$$

The integral in Eq. (4.56) becomes

$$[J^{-1}]_{l_1^2=m^2,l^2_2=m^2,l_3^2=M^2,l_4^2=M^2}. \quad (4.59)$$

The value for this is resolved explicitly by using the relation

$$[\det l_{i\mu}]^2=\det l_\mu\cdot l_\nu, \quad (4.60)$$

so that

$$J=2^4[\det l_\mu\cdot l_\nu]^{1/2}. \quad (4.61)$$

We delete the common R-matrix factors and write the spectral function in the form

$$\rho=\frac{-eG^2M^2m^2\Gamma}{16\pi}[J^{-1}]_{l_1^2=m^2,\ldots}. \quad (4.62)$$

We shall obtain the mass shell values for $l_\mu l^\nu$ by evaluating the quantities

$$(l_\mu\pm l_\nu)^2=\lambda^2, \quad (4.63)$$

so that

$$2l_\mu l^\nu=\lambda^2\mp(l_\mu^2+l_\nu^2). \quad (4.64)$$

When l_μ and l_ν meet at a common vertex, λ^2 is the square of the external particle mass entering that vertex. When l_μ and l_ν are not adjacent, then λ^2 will be one of the scalar invariants s, t, or u.

Since the cross term in the quadratic in Eq. (4.64) contains a factor of 2, it is convenient to calculate

$$\det l_\mu l^\nu=2^{-4}\det(2l_\mu l^\nu). \quad (4.65)$$

The topology represented in Fig. 9 and the masses of the particles involved are put into the determinant indicated above. Note that Fig. 9 represents both amplitudes depicted in Figs. 6(a) and 6(b). The determinant has the form

$$\det{}_{\text{ex}}=(2^{-4})\begin{vmatrix} M2^2 & 2M^2-D^2 & M^2+m^2-t & m^2\\ 2M^2-D & 2M^2 & m^2 & M^2+m^2-u\\ M^2+m^2-t & m^2 & 2m^2 & 2m^2\\ m^2 & M^2+m^2-u & 2m^2 & 2m^2\end{vmatrix}, \quad (4.66)$$

where the subscript "ex" means "exchange." Henceforth, the pion mass will be taken equal to one, but in some cases we will retain powers of m to denote units. All other energies are to be considered in pion units. After suitable change of variables and manipulations in the determinant, one finds

$$\det{}_{\text{ex}}(t,u)=(m^8/16)B_{\text{ex}}(t,u), \quad (4.67)$$

where

$$B_{\text{ex}}(t,u)\rightarrow B_{\text{ex}}(y,z)$$

and

$$B_{\text{ex}}(y,z)=[(y+z-yz)^2-4\theta yz-4M^2(y^2+z^2)]. \quad (4.68)$$

In the above we have used

$$y=t-M^2,\quad z=u-M^2,\quad \theta=2M^2-D^2. \quad (4.69)$$

Insertion of (4.67) into Eq. (4.62) yields

$$\rho_{t,u}=-(e\Gamma G^2/64\pi)(M^2/m^2)[B_{\text{ex}}(t,u)]^{-1/2}. \quad (4.70)$$

Calculation of the rescattering spectral functions may be completed using a similar procedure. Write the fourth-order amplitudes corresponding to the processes depicted in Figs. 5(a) and 5(b). Use the equivalent projection technique to isolate that part of the amplitude associated with I_{12}. The only differences that arise are due to the inclusion of the nucleon electromagnetic vertex and the fact that both neutral and charged pions are exchanged.

The integration over four-momenta is transformed in the same way, and the determinants are found to be

$$\det{}_{\text{rs}}(s,v)=(m^8/16)B_{\text{rs}}(s,v), \quad (4.71)$$

where $v=t$ or u, and the subscript "rs" means "rescattering." Note that for $t\rightarrow u$ $\det_{\text{rs}}(s,t)\rightarrow\det_{\text{rs}}(s,u)$. Now

$$B_{\text{rs}}(x,v)=v(b_v\theta-2M^2a_v)-x[2M^2c_v+b_v(v-1)]\quad\text{for}\quad v=y\text{ or }z. \quad (4.72)$$

Here

$$x=s-D^2,\qquad b_v=x(1-v)\theta+v,$$
$$a_v=x+2M^2v,\quad c_v=2x+v. \quad (4.73)$$

The spectral functions are

$$\rho_{s,v}=-(\mu_p-\mu_n)(e\Gamma G^2/64\pi)(M^3/m^3)\times[B_{\text{rs}}(s,v)]^{-1/2}, \quad (4.74)$$

where $v=t$ or u.

Several differences are observed in a comparison of the exchange and rescattering spectral functions. One sees that $\rho_{s,t}$ and $\rho_{s,u}$ contain a factor $(\mu_p-\mu_n)$ which $\rho_{t,u}$ does not. Also, the rescattering diagrams with an internal structure of three nucleons and a pion generate spectral functions with a factor $(M^3m)/m^4$. The exchange diagrams with an internal structure of two nucleons and two pions produce spectral functions with a factor $(M^2m^2)/m^4$.

Perhaps the simplest physical argument for this difference is prompted by consideration of the relative momenta of mesons and nucleons involved in the photodisintegration process. The magnitudes of the quantities M^2m^2 and M^3m should be taken as indicative of the qualitative behavior of the propagator-derived *denominator* in the amplitude. The mesons should reflect their lighter mass properties in the accompnaying momentum space description of the amplitude. The above behavior confirms an earlier hypothesis about the exchange current effects in photomagnetic amplitudes.

We may now locate the region in which the spectral functions do not vanish. These regions are defined by setting the quadratic forms B equal to zero.

Observe that $\rho_{t,u}$ is symmetric about the line $y=z$ $(t=u)$, and that $\rho_{s,t}$ and $\rho_{s,u}$ are mirrored about the same line. Secondly, one may see that for increasing values of the magnitude of s, the boundaries of all the spectral functions are asymptotic to lines in t and u which correspond to the regular threshold, i.e., for $t=u=(M+1)^2$.

We solve the biquadratic forms for one invariant in terms of the other to learn the details of the boundary. We find that $\rho_{t,u}$ has a zero on the $t=u$ line at $t=M^2+2+4\gamma$. We also find that $\rho_{s,t}$ and $\rho_{s,u}$ are tangential to this line. If we recall the results of the calculation of the anomalous threshold in t and u, we note a discrepancy. It appears that the zero of the spectral function and the anomalous threshold coincide on the line $t=u$. However, we must remark that the zero of the spectral function was calculated using the deuteron mass as

$$D^2=4M^2-4\gamma^2, \tag{4.75}$$

whereas the exact relation is

$$D^2=4M^2-4\gamma^2+B^2. \tag{4.76}$$

If one recalculates the zero of the spectral function and the anomalous threshold using the exact relation Eq. (4.76), one finds that the two points do not coincide. The threshold occurs closer to the physical region. If this were not the case—if the zero of the spectral function "preceded" the anomalous threshold—it would indicate that the singularity function is complex. In this instance the spectral function has a cusp, i.e., a discontinuity in the slope of the Landau curve. When this condition holds, the Mandelstam representation is invalid.

All three spectral functions are tangential to the lines $t=u=M^2+2+4\gamma$. As we let t and u increase, we find that the spectral functions' boundaries are asymptotic to those values for t and u defined by the regular threshold, i.e., $t=u=(M+1)^2$.

The boundaries of the fourth-order spectral functions for exchange and rescattering are shown in Fig. 7 together with other features of the scattering process, which we have discussed previously. In addition we have pictured the results of a similar calculation to find spectral functions for processes with intermediate states featuring exchange particles of *double* the pion mass. This device serves to show details of the scale we have chosen and to emphasize that section of the left-hand cut which is closest to the physical region and upon which the one-pion processes alone are important. We shall henceforth confine our interest to this portion of the cut, which is the section between the one-pion anomalous and regular thresholds.

The remaining contribution to the left-hand cut which we wish to treat is that due to the deuteron vertex properties depicted in Fig. 3(d). This graph is the means by which the nonasymptotic shape of the deuteron wave function is introduced nonrelativistically. One might treat such contributions in a consistent way by using the correct form factors in the description of the Born amplitudes depicted in Figs. 2(b) and 2(c).

However, we may estimate the contribution of these properties in a way compatible with the treatment of the exchange and rescattering corrections. The procedure is as follows: Write the Feynman amplitudes for the processes indicated by Fig. 3(d). Utilize the projection technique and the mass shell properties of the vertices to isolate the part of the amplitude associated with I_{12}. Calculate the discontinuity function of the third-order vertex using external momenta as d^μ, p^μ, or n^μ, and t or u. This function is

$$B_3=\tfrac{1}{4}[v^2-2v(D^2+M^2)+(D^2-M^2)^2]^{-1/2} \quad \text{for} \quad v=t \text{ or } u. \tag{4.77}$$

For $t=u$, the factor projected out of the amplitude is $[bG^2(M^3/m^3)]/64\pi$.

Our approximation will be to treat the amplitudes with the expanded deuteron vertex on the mass shell, but multiplied by a discontinuity function which partially accounts for the influence of the intermediate nucleon off the mass shell and the expanded vertex. Let

$$\rho_V=(\mu_p-\mu_n)(e\Gamma G^2/64\pi)(M^3/m^3)[B_3(v)]^{-1/2} \quad \text{for} \quad v=t=u. \tag{4.78}$$

We shall use this as an approximation to a single spectral function to calculate the contribution of the expanded deuteron vertex to the imaginary part of the amplitude on the region of interest in the left-hand cut.

We may now use the spectral functions to derive the imaginary part of the amplitude on the left-hand cut. This will be used to modify the input of the integral equation derived from the photomagnetic dispersion relation. The new contributions to the input will be denoted by A_{ex}, A_{rs}, and A_V. It is the imaginary parts of these that enter the dispersion relation. As before, we shall treat the exchange contribution in considerable detail and draw upon the method to describe the corresponding properties of the rescattering and vertex contributions.

Within the framework of the Mandelstam representation, we write

$$\mathrm{Im}A_{\mathrm{ex}}(s)=\mathrm{Im}\frac{1}{\pi^2}\int\int\frac{\bar{\rho}_{t'u'}dt'du'}{(t'-t-i\epsilon)(u'-u-i\epsilon)}, \qquad (4.79)$$

where we have scaled the amplitude by removing the factor $E=\pi e(\mu_p-\mu_n)\Gamma$ in order to achieve a result consistent with Eqs. (4.13), (4.24), and (4.26). Using ρ_{tu} as defined in Eq. (4.62), we wsite

$$\delta_{tu}=E\bar{\rho}_{tu}=Er_{tu}B_{\mathrm{ex}}^{1/2}. \qquad (4.80)$$

The limits of integration in Eq. (4.79) are defined by the boundaries of the spectral functions. We denote them as $t_\pm$ and $u_\pm$.

We see that $\mathrm{Im}A_{\mathrm{ex}}$ is a function of s (or ν) because we integrate along lines of constant t and u which specify the limits and define the location on the cut across which we calculate the discontinuity. Since $s+t+u=$ constant, a choice of t and u specifies the value of s for which $\mathrm{Im}A_{\mathrm{ex}}$ is calculated (See Fig. 10). In terms of t and u we may write

$$\begin{aligned}B_{\mathrm{ex}}(t,u)=[t+u-2M^2-(t+M^2)(u+M^2)]^2\\ -4\theta(t-M^2)(u-M^2)\\ -4M^2[(t-M^2)^2+(u-M^2)^2]. \qquad (4.81)\end{aligned}$$

Observe the symmetries

$$B_{\mathrm{ex}}(t,u)=B_{\mathrm{ex}}(u,t) \qquad (4.82)$$

$$t_+(s,u_0)=u_+(s,t_0)\,,\quad t_-(s,u_0)=u_-(s,t_0)\,. \qquad (4.83)$$

To find the limits explicitly, set $B_{\mathrm{ex}}(t,u_0)=0$ and solve for $t_\pm(u_0)$. Similarly, one may set $B_{\mathrm{ex}}(t_0,u)=0$ and solve for $u_\pm(t_0)$. Another important feature of the spectral function is that

$$B_{\mathrm{ex}}(t_A,u_A)=0\,, \qquad (4.84)$$

where

$$t_A=u_A=M^2+2+4\gamma \text{ (pion units)}. \qquad (4.85)$$

Using Eqs. (4.80), (4.82), and (4.83) in Eq. (4.79), we find

$$\mathrm{Im}A_{\mathrm{ex}}(s)=\frac{2r_{tu}}{\pi}P\int_{u_-(s,t_0)}^{u_+(s,t_0)}\frac{du}{(u-u_0)[B_{\mathrm{ex}}]^{1/2}}, \qquad (4.86)$$

where we have expanded the complex denominators in Eq. (4.79) using the relation

$$\frac{1}{x'-(x\pm i\epsilon)}=P\frac{1}{x'-x}\pm i\pi\delta(x'-x)\,. \qquad (4.87)$$

We transform the variables using Eq. (4.69) and setting

$$y-y_0=Y\,,\quad\text{and}\quad z-z_0=Z\,. \qquad (4.88)$$

We set $y_0=z_0=\text{constant}=D^2-s=-2M\nu$ fixed.

Thus,

$$\begin{aligned}\mathrm{Im},A_{\mathrm{ex}}(s)&=\frac{2r_{tu}}{\pi}\int_{Z_-}^{Z_+}\frac{dZ}{Z[c_1+c_2Z+c_3Z^2]^{1/2}}\\ &=\frac{2r_{tu}}{\pi}\sinh^{-1}\left[\frac{2c_1+c_2Z}{Z[4c_1c_3-c_2^2]^{1/2}}\right]_{z_-}^{z_+}\text{ for } c_1>0\,, \qquad (4.89)\end{aligned}$$

where

$$\begin{aligned}c_1&=16H^2[(1+H)^2-4\gamma^2]\,,\\ c_2&=-8H[(1+H)(1+2H)-4\gamma^2]\,, \qquad (4.90)\\ c_3&=[(1+2H)^2-4M^2]\,,\end{aligned}$$

and

$$H=M\nu=(s-D^2)/4\,. \qquad (4.91)$$

Since the principal part of the $\sinh^{-1}$ may be represented as

$$\sinh^{-1}A=\ln[(1+A^2)^{1/2}+A]\,, \qquad (4.92)$$

we find

$$\mathrm{Im}A_{\mathrm{ex}}=\frac{2r_{tu}}{\pi c_1}\ln\left[\frac{(T_-^2+1)^{1/2}+T_-}{(T_+^2+1)^{1/2}+T_+}\right], \qquad (4.93)$$

where

$$T_\pm=[2c_1+c_2Z_\pm][(Z_\pm^2)(4c_1c_3-c_2^2)]^{-1/2}. \qquad (4.94)$$

Evaluating $(T_\pm^2+1)^{1/2}$, we can show

$$\begin{aligned}4c_1^2+4c_1c_2Z_\pm+c_2^2Z_\pm^2+Z_\pm^2(4c_1c_3-c_2^2)\\ =4c_1[c_1+c_2Z_\pm+c_3Z_\pm^2]. \qquad (4.95)\end{aligned}$$

But $Z_\pm$ are roots of the quadratic form in Eq. (4.95); so we find that the argument of the radical is zero. More simply then,

$$\mathrm{Im}A_{\mathrm{ex}}(s)=\frac{2r_{tu}}{\pi c_1}\ln\left[\left(\frac{Z_+}{Z_-}\right)\frac{2c_1+c_2Z_-}{2c_1+c_2Z_+}\right]. \qquad (4.96)$$

In the argument of the logarithm in Eq. (4.93), reduce the common factors, and multiply the numerator and denominator by c_3. The rseult is

$$\mathrm{Im}A_{\mathrm{ex}}(H)=\frac{2r_{tu}}{\pi c_1}\ln\left[\left(\frac{Z_+}{Z_-}\right)\frac{(1+H)^2-4\gamma^2(1+2H)^2-4M^2+\bar{Z}_-(1+H)(1+2H)-4\gamma^2}{(1+H)^2-4\gamma^2(1+2H)^2-4M^2+\bar{Z}_+(1+H)(1+2H)-4\gamma^2}\right], \qquad (4.97)$$

where

$$Z_\pm=-2H\frac{(40-1-2H)\pm2M[4H^2+48H+48M^2+24]^{1/2}-[(1+2H)^2-4M^2]}{[(1+2H)^2-4M^2]} \qquad (4.98)$$

and

$$\bar{Z}_{\pm}(c_3/4H)Z_{\pm}. \tag{4.99}$$

From this form of the argument of the logarithm, one can clearly see that the exchange contribution to the imaginary part of the amplitude vanishes at the anomalous and regular thresholds.

We now account for the rescattering contributions to the discontinuity function in this region. We begin by stating

$$\mathrm{Im}A_{\mathrm{rs}}=\mathrm{Im}\frac{1}{\pi^2}\int\int\frac{\bar{\rho}_{s't'}ds'dt'}{(s'-s)(t'-t)}+\int\int\frac{\bar{\rho}_{s'u'}ds'du'}{(s'-s)(t'-t)}. \tag{4.100}$$

Again,

$$\rho_{st}=E\bar{\rho}_{st}=Er_{st}[B_{\mathrm{rs}}(s,t)]^{-1/2}. \tag{4.101}$$

From Eq. (4.74) we note that $\rho_{s,t}\leftrightarrow\rho_{s,u}$, if $t\rightarrow u$, i.e., the rescattering or cross channel spectral functions have the same functional form in t and u. They are symmetric about the line defined by the condition $t=u$. The limits of integration are determined in the same way as in the exchange calculation. One may note a qualitative difference in the exchange and rescattering contributions. The ordering of the analogous limits, that is, those denoted by "+" or "−", is reversed. The result is that the exchange and rescattering contributions are of opposite sign and tend to cancel.

Having established this qualitative difference, let us now find the magnitude of the rescattering contribution. As before

$$\mathrm{Im}A_{\mathrm{rs}}=\frac{1}{\pi}\left[P\int\frac{\bar{\rho}_{s't}ds'}{(s'-s)}+P\int\frac{\bar{\rho}_{st'}dt'}{(t'-t)}+P\int\frac{\bar{\rho}_{s'u}ds'}{(s'-s)}+P\int\frac{\bar{\rho}_{su'}du'}{(u'-u)}\right]. \tag{4.102}$$

Note that the integrals in which s is constant will vanish in the region of interest, since here $s<0$ and the denominators $[B_{\mathrm{rs}}(s=\text{const.}, t' \text{ or } u')]^{1/2}$ do not vanish. Then, due to the t, u symmetry,

$$\mathrm{Im}A_{\mathrm{rs}}=-\frac{2}{\pi}r_{st}P\times\int_{s-}^{s+}\frac{ds'}{(s'-s)[B_{\mathrm{rs}}(s', t=u=\text{const})]^{1/2}} \tag{4.103}$$

$$\mathrm{Im}A_{\mathrm{rs}}(H)=-\frac{2r_{st}}{\pi}\frac{1}{d_1}\ln\left[\left(\frac{\bar{d}_2+MV}{\bar{d}_2-MV}\right)\times\left(\frac{\bar{d}_1d_3-\bar{d}_2{}^2+\bar{d}_2MV}{\bar{d}_1d_3-\bar{d}_2{}^2-\bar{d}_2MV}\right)\right]. \tag{4.104}$$

The difference in sign between Eqs. (4.104) and (4.93) has been discussed. The differences in form result because the "constant term" in the quadratic form in the integrand of Eq. (4.103) is <0. In Eq. (4.104) we have used

$$d_1(H)=16H^2\bar{d}_1(H)=16H^2[4H^2+4H(HM^2-2\gamma^2)+1-4\gamma^2(HM^2-2\gamma^2)],$$
$$d_2(H)=8H\bar{d}_2(H)=8H[4H^2+2H(2+M^2-2\gamma^2)+(1-2M^2-2\gamma^2)], \tag{4.105}$$
$$d_3(H)=(1+2H)^2-4M^2)=C_3(H)\ [\text{see Eq. (5.89)}],$$

and

$$MV=2M^2[H^2+2+(1-4\gamma^2)]^{1/2}. \tag{4.106}$$

Examination of the argument of the logarithm in Eq. (4.104) shows that $\mathrm{Im}A_{\mathrm{rs}}$ also vanishes at the anomalous and regular thresholds. We may now neglect $\mathrm{Im}A_{\mathrm{rs}}$ in Fig. 10 because calculation demonstrates that in the region $H\leq M\nu_{1A}$

$$\mathrm{Im}A_{\mathrm{rs}}\cong 10^{-2}\,\mathrm{Im}A_{\mathrm{ex}}. \tag{4.107}$$

In similar fashion we define

$$\mathrm{Im}A_V=\mathrm{Im}\frac{1}{\pi}\int\frac{dv'\bar{\rho}v}{v'-v}, \tag{4.108}$$

where

$$\rho_v=E\bar{\rho}_v=Er_v[B_3(v)]^{-1/2}. \tag{4.109}$$

We have taken the variable v as representative of both t and u, and indicative of the fact that ρ_v represents contributions from both diagrams implied by Fig. 3(d). We utilized the equality of t and u to produce the similarity in the electromagnetic factors appearing in Eq. (4.74). This is not possible if $t\neq u$.

We find

$$\mathrm{Im}A_\nu(v)=r_v[B_3(v)]^{-1/2}. \tag{4.110}$$

For those values of $v=t=u$ for which $H<M\nu_{1A}$, we find that

$$\mathrm{Im}A_\nu\sim 10^{-1}\,\mathrm{Im}A_{\mathrm{rs}}, \tag{4.111}$$

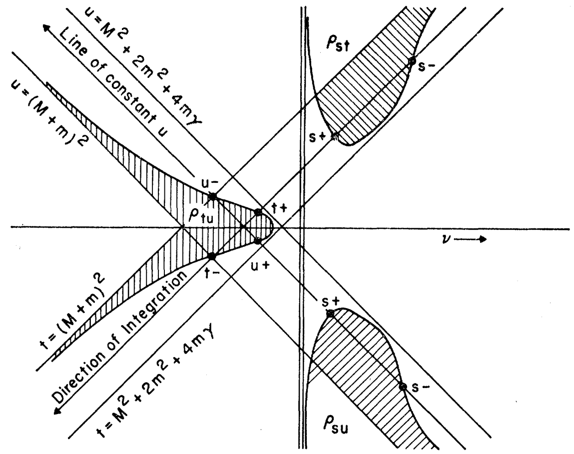

FIG. 10. Integration in the anomalous tip.

and thus the contribution from the expanded deuteron vertex may be neglected in this region.

Comparison of the magnitudes in Eq. (4.107) allows us to set

$$\mathrm{Im}A_{\mathrm{tip}}\approx \mathrm{Im}A_{\mathrm{ex}} \tag{4.112}$$

in the "anomalous tip."

For the integral over the left-hand cut we now take

$$\frac{1}{\pi}\int_{-\infty}^{\nu_{1A}}\frac{\mathrm{Im}A(\nu')d\nu'}{(\nu'-\nu)}=I_{\mathrm{lhc}}(\nu)\doteq\frac{1}{\pi}\int_{\nu_{\mathrm{IR}}}^{\nu_{1A}}\frac{\mathrm{Im}A_{\mathrm{ex}}(\nu')}{\nu'-\nu}. \tag{4.113}$$

It is possible to treat this approximation of the integral of I_{lhc} exactly using Spence functions.[41] However, we have indicated that because the one-pion exchange section of the cut is fairly short, we can approximate the above modification of the input function of the integral equation derived from I_{lhc} by a δ function. To fit the residue and position of the pole yielding this δ function, we set

$$I_{\mathrm{lhc}}(\nu)=\bar{R}/(\nu+\nu_p)\,,\qquad I_{\mathrm{lhc}}'(\nu)=-\bar{R}/(\nu+\nu_p)^2. \tag{4.114}$$

Here, $\bar{R}$ is the residue and ν_p the location of the pole.

Consistent with this approximation, we calculate $I_{\mathrm{lhc}}(\nu)$ and $I_{\mathrm{lhc}}'(\nu)$ for $\nu=$constant. The value of this constant is physically significant inasmuch as it serves to locate the interaction pole and should coincide with the region where the exchange current is important. We choose $\nu=B$ to locate the pole at threshold. This energy is within a few keV of the energy corresponding to thermal neutron capture. It can be shown that variation of ν over an interval as large as 1 MeV around threshold will have virtually no effect on the ultimate location of the pole.

Equation (4.113) takes the form

$$I(\nu)=\frac{2r_{tu}}{\pi^2}\int_{\nu_{\mathrm{RI}}}^{\nu_{1A}}\frac{d\nu'\ln[(Z_+/Z_-)(2c_1+c_2Z_-)/(2c_1+c_2Z_+)]}{(\nu'-\nu)4M\nu'[(1+M\nu')^2-4\gamma^2]^{1/2}}=\frac{\bar{R}}{\nu+\nu_p}. \tag{4.115}$$

Taking the derivative indicated in Eq. (4.14) produces

$$\frac{d}{d\nu}I(\nu)=I'(\nu)=\frac{2r_{tu}}{\pi^2}\int_{\nu_{\mathrm{IR}}}^{\nu_{\mathrm{IA}}}\frac{d\nu'\ln[(Z_+/Z_-)(2c_1+c_2Z_-)/(2c_1+c_2Z_+)]}{(\nu'-\nu)^2[(1+M\nu')^2-4\gamma^2]^{1/2}4M\nu'}=\frac{-\bar{R}}{(\nu+\nu_p)^2}. \tag{4.116}$$

The integrals are scaled using Eq. (4.91) and calculated numerically. The results of the integration are

$$I=(2r_{tu}/\pi^2)(2.533\times10^{-2})\,,\qquad I'=(2r_{tu}/\pi^2)(7.134\times10^{-2})m^{-1}. \tag{4.117}$$

In the above, all energetic quantities are in pion units.

The first result we wish to exploit is that the position of the pole is fixed by the ratio of I and I'. We see

$$\nu_p=-[I/I')+\nu]=-0.371\ (\text{pion units})=-50.5\ \text{MeV}. \tag{4.118}$$

Next, note $\bar{R}$ has the same sign as ν_p. This indicates an enhancement of the amplitude and an increase in the cross section.

Using Eq. (4.80) to define r_{tu}, we find

$$\frac{2r_{tu}}{\pi^2}=\frac{G^2M^2}{32\pi^4(\mu_p-\mu_n)}=0.556. \tag{4.119}$$

Here we have taken $G^2=16\pi M^2f^2$ when f^2 is the renormalized coupling constant. We find $G^2=180$. Thus

$$\bar{R}=(\nu+\nu_p)I=-0.68\ \text{MeV}. \tag{4.120}$$

This point is shown in Fig. 9. It is seen from a comparison of the residues of the exchange pole and the correction pole at the energy fixed in Eq. (4.113), that the exchange pole, when substituted into the integral equation, will indeed resolve the existing discrepancy between the Born cross section and the experimental value. Furthermore, the arguments we have presented lead us to state that the exchange contribution is the only correction required in the threshold region. The rescattering is too small to affect the threshold values and we have utilized the effective range approximation for the $^1S_0$ phase shift. The usage insures a description of the over-all rescattering effects.

Conclusions

The development has shown that the inclusion of higher-order corrections associated with the meson exchange current improves the agreement between the experimental and theoretical values of the photodisintegration cross section near threshold.

The deuteron's unique parity, spin, and isospin relations are antecedents of the particular momentum dependence of the $M1$ and $E1$ amplitudes. The predominance of the $M1$ amplitude at threshold, coupled with the proximity of the exchange singularities and magnitude of the corrections attributable to them, is vital to the result. This proximity was found to be the result of the very small binding energy of the deuteron, which promotes an anomalous threshold. This correction was found by calculating the difference in the exchange discontinuity function across the cut only in the anomalous tip region of the exchange spectral function. We also found the contributions from the rescattering and

[41] K. Mitchell, Phil. Mag. 40, 351 (1949).

d-np vertex. These were negligible compared to the exchange contributions.

The cross channel structure of the Mandelstam representation which leads to the construction of the exchange spectral function, from which the information about the imaginary part of the amplitude in the unphysical region was derived, provides a format for the calculation of the relativistic meson exchange effects in an otherwise nonrelativistic problem.

We stated that the general T-matrix element, a 12-fold sum of Lorentz covariants, must be gauge and spatially invariant and must obey the generalized Pauli prinicple. Since we have treated the twelve Lorentz covariants as independent, we have required that each individual invariant obey the spatial, gauge, and Pauli restrictions.

Our efforts were confined to a claculation of the amplitude very close to the physical threshold. We saw that in this region $^1D_2$ amplitude could be neglected. This approximation provides a great simplification in the form of the dispersion relation. A similar simplification was made when we showed the $^3S_1$ amplitude must be much smaller than the $^1S_0$.

To obtain solutions to the integral equation, we assumed that the amplitude and the final n-p phase shift were bounded at large energies as one proceeded in any radial direction in the complex p^2 plane. In this light it might seem inconsistent to use the effective range approximation for the phase shift, since it does not have the high-energy boundedness properties. However, the subtracted form of the dispersion relation features a denominator that seems to provide rapid enough growth to compensate for the more slowly increasing approximation to the phase shift. In further calculations we might suggest that one use an analytic approximation to one of the experimental phase-shift solutions, for instance, the YLAM solution of Breit *et al.*[42]

Finally, we comment about our use of the d-np vertex function in the composition of the fourth-order amplitude. We have relied heavily on mass shell restrictions to convert the outgoing nucleons defined in this vertex to intermediate propagators. Thus, with a suitable change of normalization, the deuteron form factors may be utilized as vertex functions. We noted that this usage seemed reasonable, since it is really just an extension of the method used to compose the Born amplitudes.

ACKNOWLEDGMENTS

The author would like to thank Professor Philip Morrison for introducing him to the subject, and to acknowledge stimulating discussions with J. L. Morrison and Professor W. Bertozzi and his experimental group. The author would also like to thank Professor H. P. Noyes for several useful communications, Professor P. T. Demos for the hospitality extended by him at the laboratory of Nuclear Science at MIT, and Professor J. Robert Oppenheimer for his generous hospitality at the Institute for Advanced Study.

APPENDIX A. THE SOLUTION OF THE INTEGRAL EQUATIONS

We wish to solve an integral equation of the form

$$A(x)=\frac{R}{x+x_p}+\alpha+\beta x+\frac{x+\gamma^2}{\pi}\int_0^\infty \frac{\tan\delta(x')A(x')dx'}{(x'+\gamma^2)(x'-x)}, \quad \text{(A1)}$$

where x_p, R, α, β, and γ^2 are real, and both γ^2 and $x_p>0$. Proper boundary conditions are $A(\infty)=\text{constant}$, $\delta(\infty)=\text{constant}$, and $\delta(0)=0$. Let

$$\phi(z)=(R/z+z_p)+\alpha+\beta z+F(z), \quad \text{(A2)}$$

$$\phi(z)=I(z)+N(z)/D(z). \quad \text{(A3)}$$

Now

$$\lim_{\epsilon\to 0}\phi(x+i\epsilon)=A(x), \quad \text{(A4)}$$

so that

$$\phi(x+i\epsilon)=[I(x+i\epsilon)+F(x+i\epsilon)]\theta x. \quad \text{(A5)}$$

Here,

$$\theta(x)=1 \quad \text{if} \quad 0<x; \quad \theta(x)=0 \quad \text{if} \quad x\leq 0.$$

Rewrite Eq. (A5) as

$$\phi(x+i\epsilon)=I(x+i\epsilon)+[N(x+i\epsilon)/D(x+i\epsilon)]. \quad \text{(A6)}$$

Define the real, analytic Omnes function (the denominator function) as

$$D(z)=\exp\left\{-\frac{z+\gamma^2}{\pi}\int_0^\infty \frac{dz'\delta(z')}{(z'+\gamma^2)(z'-z)}\right\} \quad \text{(A7)}$$

and see

$$D(x\pm i\epsilon)=\exp\left\{-\frac{x+\gamma^2\pm i\epsilon}{\pi}\times\int\frac{\delta(z')dz'}{(z'+\gamma^2)(z'-z\mp i\epsilon)}\right\}. \quad \text{(A8)}$$

We expand Eq. (A8) using Eq. (4.87) and write

$$D(x\pm i\epsilon)=\exp\left\{-\frac{x+\gamma^2}{\pi}\int\frac{\delta(x')}{x'+\gamma^2}\times\left[\pm i\pi\delta(x'-x)+P\left(\frac{1}{x'-x}\right)\right]dx'\right\}. \quad \text{(A9)}$$

Now

$$\frac{x+\gamma^2}{\pi}\int\frac{dx'\delta(x')}{x'+\gamma^2}P\left(\frac{1}{x'-x}\right)=\frac{x+\gamma^2}{\pi}P\int\frac{dx'\delta(x')}{(x^1+\gamma^2)(x'-x)}=\tau(x). \quad \text{(A10)}$$

G. Breit, M. H. Hull, Jr., K. E. Lassila, and K. D. Pyatt, Jr., Phys. Rev. **120**, 2227 (1960).

From Eqs. (A9) and (A10) one finds

$$D(x\pm i\epsilon)=\exp[-\tau(x)\mp\delta(x)]. \quad \text{(A11)}$$

This result in turn prompts us to write

$$\frac{N(x+i\epsilon)e^{-i\delta}}{D(x+i\epsilon)}-\frac{N(x-i\epsilon)e^{i\delta}}{D(x-i\epsilon)} =e^{\tau(x)}[N(x+i\epsilon)-N(x-i\epsilon)], \quad \text{(A12)}$$

from which we see

$$N(x+i\epsilon)-N(x-i\epsilon) =2i\sin\delta e^{-\tau(x)}\left[\alpha+\beta x+\frac{R}{x+x_p}\right] \quad \text{(A13)}$$

and

$$F(-\gamma^2)=N(-\gamma^2)/D(-\gamma^2)=0. \quad \text{(A14)}$$

It must be the case that $N(-\gamma^2)=0$.

The general solution for the difference of an analytic function across a cut ζ, for example a function given by

$$N_+-N_-=f(z),$$

is

$$N(z)=\frac{1}{2\pi i}\int_\zeta\frac{f(z')dz'}{z'-z}, \quad \text{(A15)}$$

which may be generalized for our subtraction as

$$N(z)=\frac{1}{2\pi i}(z+\gamma^2)\int_\zeta\frac{f(z')dz'}{(z'+\gamma^2)(z'-f)}. \quad \text{(A16)}$$

Thus

$$N(z)=\frac{1}{\pi}(z+\gamma^2)\int_\zeta\frac{\sin\delta(z')e^{-\tau(z')}}{(z'+\gamma^2)(z'-z)} \times\left[\alpha+\beta z'+\frac{R}{z'+z_p}\right]dz'. \quad \text{(A17)}$$

Now from the original definition of $\phi(z)$, namely Eq. (A2), we have

$$\phi(x+i\epsilon)\to I(x)+e^{\tau(x)}e^{i\delta(x)} \times\left[\frac{x+\gamma^2}{\pi}\int dx'\frac{\sin\delta(x')e^{-\tau(x')}I(x')}{(x'+\gamma^2)}\right] \times\left[i\pi\delta(x'-x)+P\frac{1}{x'-x}\right] \quad \text{(A18)}$$

and

$$\phi(x+i\epsilon)\underset{\epsilon\to0}{\longrightarrow}A(x)=I(x) +e^{\tau}e^{i\delta}\left\{\frac{x+\gamma^2}{\pi}\left[\frac{i\pi\sin\delta(x')e^{-\tau(x')}I(x')}{(x+\gamma^2)} +P\int_0^\infty\frac{\sin\delta e^{-\tau}I(x')dx'}{(x'+\gamma^2)(x'-x)}\right]\right\}. \quad \text{(A19)}$$

Combining the terms and simplifying yields

$$A(x)=e^{i\delta(x)}I(x)\cos\delta(x) +e^{\tau(x)}\frac{x+\gamma^2}{\pi}P\int_0^\infty\frac{\sin\delta e^{-\tau}I(x')dx'}{(x'+\gamma^2)(x'-x)}. \quad \text{(A20)}$$

The boundary conditions must still be matched. To this end we note that we could add any solution of the homogeneous equation

$$A_0(x)=\frac{x+\gamma^2}{\pi}P\int\frac{\tan\delta(x')A(x')}{(x'+\gamma^2)(x'-x)}dx'.$$

We find such a solution using the method outlined above. Note that the "denominator" function must be the same in each instance, since the same physical singularities, that is, the right-hand cut properties, must be duplicated. As defined above

$$F_0(z)=\frac{N_0(z)}{D_0(z)}=\frac{z+\gamma^2}{\pi}\int_{\text{cut}}\frac{\tan\delta A(z')dz'}{(z'+\gamma^2)(z'-z)}. \quad \text{(A21)}$$

We now show

$$\lim_{\epsilon\to0}N_0(x+i\epsilon)-N_0(x-i\epsilon)=0. \quad \text{(A22)}$$

In an obvious notation

$$N_{0+}-N_{0-}=F_{0+}D_{0+}-F_{0-}D_{0-}$$
$$=e^{-\tau}[e^{-i\delta}F_{0+}-e^{i\delta}F_{0-}]$$
$$=e^{-\tau}e^{-i\delta}\left[i\tan\delta(x)A_0(x)+\frac{x+\gamma^2}{\pi}P\int_0^\infty\frac{\tan\delta A(x')dx'}{(x'+\gamma^2)(x'-x)}\right]-e^{i\delta}\left[-i\tan\delta A_0(x)+\frac{x+\gamma^2}{\pi}P\int_0^\infty\frac{\tan\delta A(x')dx'}{(x'+\gamma^2)(x'-x)}\right]$$
$$=e^{-\tau}\left[2i\cos\delta\tan\delta A_0(x)-2i\sin\delta\frac{x+\gamma^2}{\pi}P\int_0^\infty\frac{\tan\delta A(x')dx'}{(x'+\gamma^2)(x'-x)}\right].$$

But

$$A_0(x)=\frac{x+\gamma^2}{\pi}P\int_0^\infty \frac{\tan\delta A(x')dx'}{(x'+\gamma^2)(x'-x)}.$$

Thus

$$N_{0+}-N_{0-}=e^{-\tau}2iA_0(\sin\delta-\sin\delta)=0. \quad \text{Q.E.D.}$$

We may state that N_0 is a whole analytic function in the z-plane except where singularities may occur at zero or infinity.

The most general solution is given by

$$\phi(z)=I(z)+\frac{N(z)}{D(z)}+\frac{P(z+\gamma^2)}{D(z)}, \quad \text{(A23)}$$

where $P(z)$ is a polynomial to be determined. The solution can be put into the form

$$A(x)=e^{i\delta}\bigg[I(x)\cos\delta+e^{\tau}\frac{x+\gamma^2}{\pi}P \times\int\frac{\tan\delta A(x')dx'}{(x'+\gamma^2)(x'-x)}+e^{\tau}P(x+\gamma^2)\bigg]. \quad \text{(A24)}$$

Now $A(x)$ must be bounded as $x\to\infty$, and since we have required $\delta(x)\to 0$ as $x\to\infty$, we find

$$\lim_{x\to\infty}\bigg[P(x+\gamma^2)e^{\tau(x)} +\left(\frac{R}{x+x_p}+\alpha+\beta x\right)\cos\delta(x)\bigg]\to \text{constant}, \quad \text{(A25)}$$

so that

$$\lim_{x\to\infty}P(x+\gamma^2) =[\text{constant}-(\alpha+\beta x)\cos\delta(x)]e^{-\tau(x)}. \quad \text{(A26)}$$

This solution with a more explicit statement of parameters is the one found in Eq. (4.30). From the statements in the body of the paper, we see

$$P(x+\gamma^2)_{x\to\infty}\to -(\alpha+\beta x)\cos\delta e^{-\tau(x)}\to 0. \quad \text{(A27)}$$

APPENDIX B. PROJECTION OF A PARTICULAR INVARIANT AMPLITUDE OUT OF THE TOTAL FEYNMAN AMPLITUDE

We shall find the following relations useful:

$$\begin{aligned} &q=(p-n)/2, \quad Q=(p+n)/2, \quad A=\gamma_\mu A^\mu=\gamma\cdot A,\\ &\mathbf{q}\doteq M, \quad \mathbf{Q}\doteq 0, \quad \gamma_5\mathbf{q}\doteq 0,\\ &\mathbf{p}\doteq M, \quad \mathbf{n}\doteq -M. \end{aligned} \quad \text{(B1)}$$

Here, the symbol $\doteq$ means equality in the Dirac sense, that is, equality between the spinors.

The invariant involved in the dispersion relation for the $M1$ singlet amplitude has the form

$$I_{12}=\frac{1}{2M}\epsilon_{\mu\nu\rho\sigma}k^\rho\gamma^\sigma\gamma^5 e^\mu U^\nu=-\frac{1}{2M}\gamma^5\epsilon_{\mu\nu\rho\sigma}k^\rho\gamma^\sigma e^\mu U^\nu. \quad \text{(B2)}$$

This can be rewritten in a more useful form if one empolys the identity

$$\gamma_5\epsilon_{\mu\nu\rho\sigma}\gamma^\sigma=\gamma_\mu\gamma_\nu\gamma_\rho-g_{\mu\nu}\gamma_\rho+g_{\mu\rho}\gamma-g_{\nu\rho}\gamma_\mu. \quad \text{(B3)}$$

For a discussion of the tensor operators, $g_{\mu\nu}$, $\sigma_{\mu\nu}$, and $\epsilon_{\mu\nu\rho\sigma}$, see Schweber.[39] Applying (B3) we find

$$-\frac{1}{2M}\gamma_5\epsilon_{\mu\nu\rho\sigma}k^\rho\gamma^\sigma e^\mu U^\nu=\mathbf{e}\mathbf{U}\mathbf{k}-(e\cdot U)\mathbf{k}-(k\cdot U)\mathbf{e}, \quad \text{(B4)}$$

so that

$$I_{12}=\frac{1}{2M}[\mathbf{U}\mathbf{e}\mathbf{k}+(k\cdot U)\mathbf{e}-(e\cdot U)\mathbf{k}]. \quad \text{(B5)}$$

Our next step is to note that any product of γ matrices may be represented in the SPAVT form as

$$\begin{aligned}[\gamma\cdots\gamma]=&[[\gamma\cdots\gamma]]I+[[\gamma\cdots\gamma\gamma_\rho]]\gamma_\rho\\ &+[[\gamma\cdots\gamma\sigma_{\mu\nu}]]\sigma_{\mu\nu}+[[\gamma\cdots\gamma\gamma_5]]\gamma_5\\ &+[[\gamma\cdots\gamma_i\gamma_\sigma\gamma_5]]i\gamma_\sigma\gamma_5.\end{aligned} \quad \text{(B6)}$$

Here $[[\gamma\cdots]]$ means $\frac{1}{4}$ Trace $[\gamma\cdots]$. Using this representation, we can show

$$\mathbf{U}\mathbf{e}\mathbf{k}=[[\mathbf{U}\mathbf{e}\mathbf{k}\gamma_\rho]]\gamma_\rho+[[\mathbf{U}\mathbf{e}\mathbf{k}\gamma_\rho\gamma_5]]\gamma_5\gamma_\rho, \quad \text{(B7)}$$

and that

$$\begin{aligned}I_{12}&=\frac{1}{2M}([[\mathbf{U}\mathbf{e}\mathbf{k}\gamma_\rho\gamma_5]])\\ &=\frac{1}{2M}[\mathbf{U}\mathbf{e}\mathbf{k}+(U\cdot k)\mathbf{e}-(U\cdot e)\mathbf{k}].\end{aligned} \quad \text{(B8)}$$

If one examines Table I of the Lorentz invariants in SG, one finds that I_{12} is the only pseudovector invariant. From this alone it is easy to see that

$$I_{12}\cdot I_j=0 \quad \text{for all } j\neq 12,$$

where again

$$I_\mu\cdot I_\nu=[[I_\mu^\dagger\cdot I_\nu]].$$

In taking these traces, one should inject the appropriate positive energy projection operators to eliminate the contribution of the negative energy spinor components. Alternatively, one could decompose the spinors to the nonrelative Pauli spinors and follow an analogous procedure.

We have not followed this procedure because it would seem that at threshold, i.e., when $p\to 0$, we will see the correct kinematical behavior even when projection operators are not included.[43] We can use (B8) to show

[43] I am grateful to J. L. Morrison for bringing this to my attention.

that

$$I_{12}^2=e^2(U\cdot k)^2/4M^2=-(U\cdot k)^2/4M^2. \quad \text{(B9)}$$

We utilize this orthogonality by adapting I_{12} as a projection operator which will, when applied to the Feynman amplitude, project out the invariant amplitude which is the coefficient of I_{12} in the summed representation of the transition matrix element.

The numerator of the Feynman amplitude in which we are interested is given in Eq. (4.46). It is

$$N\simeq -e\cdot(l_1+l_2)\gamma_5(\boldsymbol{l}_3+M) \times[\tilde{F}\boldsymbol{U}+(\tilde{G}/M)(l_3\cdot U)]\gamma_5(\boldsymbol{l}_4+M). \quad \text{(B10)}$$

To simplify this we employ some of the relations of constraint enjoined by the four-momenta conserving δ functions operating at every vertex in Fig. 9. We find

$$d=l_3+l_4,\quad l_3-n=l_2,\quad l_2+k=l_1,\quad l_1+l_4=p. \quad \text{(B11)}$$

We may also derive some additional quantities which will prove useful.

$$\begin{aligned} e\cdot l_1&=e\cdot k+e\cdot l_2=e\cdot l_2\\ U\cdot d&=0=p\cdot U+n\cdot U\\ k\cdot l_1&=k\cdot l_2+k\cdot k=k\cdot l_2\\ l_1^2&=l_2^2=m^2. \end{aligned} \quad \text{(B12)}$$

The quantity described in Eq. (B10) may be simplified by observing that the definition for a product in our invariant space calls for taking traces. The trace of the product of an odd number of γ matrices is zero. We need consider only those parts of N which when multiplied by I_{12} will combine to yield an even number of γ matrices. We may also take advantage of the simplifications present in Eq. (B12) to write

$$N\simeq -2(e\cdot l_1)[\tilde{F}\boldsymbol{l}_1\boldsymbol{U}\boldsymbol{l}_2-(\tilde{G}/2M)(l_3\cdot U)2M\boldsymbol{l}_2]. \quad \text{(B13)}$$

Then

$$I_{12}\cdot N\simeq\frac{1}{2M}2(e\cdot l_1)[[\{\boldsymbol{k}\boldsymbol{e}\boldsymbol{U}+(U\cdot k)\boldsymbol{e}-(U\cdot\epsilon)\boldsymbol{k}\} \times\{\tilde{F}\boldsymbol{l}_1\boldsymbol{U}\boldsymbol{l}_2-\tilde{G}(l_3\cdot U)\boldsymbol{l}_2\}]]. \quad \text{(B14)}$$

Manipulation of the γ matrices leads to the result

$$I_{12}\cdot N=\frac{1}{M}(e\cdot l_1)\tilde{F}(U\cdot k) \times[(e\cdot l_1)(U\cdot l_2)-(e\cdot l_2)(U\cdot l_1)]. \quad \text{(B15)}$$

Using Eqs. (B12) and (B11) again, we find

$$\begin{aligned} I_{12}\cdot N&=(1/M)(e\cdot l_1)^2(-k\cdot U)\tilde{F}\\ &=(1/M)(e\cdot l_1)^2(U\cdot k)^2\Gamma(1+\Delta). \end{aligned} \quad \text{(B16)}$$

We devide Eq. (B16) by the normalization factor I_{12}^2 to find

$$\frac{I_{12}\cdot N}{I_{12}^2}=-4M(e\cdot l_1)^2\Gamma(1+\Delta). \quad \text{(B17)}$$

We need now only calculate the quantity $(e\cdot l_1)^2$ on the mass shell to completely evaluate the invariant amplitude corresponding to I_{12}.

A straightforward but somewhat tedious method for evaluating scalar products is to expand them in terms of four orthonormal four-vectors which one can construct from the external independent four-vectors involved in the problem, i.e., d^μ, k^μ, n^μ, and p^μ. However, only three of these may be taken as independent, so one must use the antisymmetric tensor to construct the fourth.

Yet, when one deals with the photon's polarization vector there is a considerable simplification. The polarization vector is spacelike and transverse. It can be written as

$$e=(e_C\pm ie_D)/\sqrt{2};\quad e^2=1- \quad \text{(B18)}$$

and

$$\begin{aligned} e\cdot l_1&=(e_C\cdot l_{1C}\pm ie_D\cdot l_{1D})/\sqrt{2},\\ (e\cdot l_1)^2&=(e\cdot l)^*(e\cdot l_1)=e_C^2l_C^2+e_D^2l_D^2,\\ (e\cdot l_1)^2&=-\tfrac{1}{2}(l_C^2+l_D^2). \end{aligned} \quad \text{(B19)}$$

But on the mass shell $l_1^2=m^2$ it must be that $-(l_C^2+l_D^2)=m^2$, since C and D denote spacelike components. Thus we may conclude

$$(e\cdot l_1)^2=\tfrac{1}{2}m^2. \quad \text{(B20)}$$

This same result is obtained when one chooses to perform the operation with the orthonormal base which we have outlined above.

The basis vectors are constructed as

$$A^\mu=\frac{Q^\mu}{|Q|};\quad B^\mu=\frac{r^\mu}{|r|};\quad C^\mu=\frac{q^\mu}{|q|};\quad D^\mu=\epsilon_{\mu\nu\rho\sigma}A^\nu B^\rho C^\sigma, \quad \text{(B21)}$$

and $r^\mu=k^\mu-\omega=-\mathbf{k}$. These are demonstrably orthonormal. By using the factorizztion $(e\cdot l)=(e\cdot A)(l\cdot A)+(e\cdot B)(l\cdot B)+\cdots$, one finds

$$(e\cdot l_1)^2=(e_C^2l_{1C}^2+e_D^2l_{1C}^2)=-\tfrac{1}{2}(l_{1C}^2+l_{1D}^2), \quad \text{(B22)}$$

and indeed the analysis projected above is verified. We do find $m^2=-(l_{1C}^2+l_{1D}^2)$. Thus Eq. (B17) reduces to

$$I_{12}\cdot N/I_{12}^2=-2m^2M\Gamma(1+\Delta). \quad \text{(B23)}$$

This is the expression found in Eq. (4.53).